universität wien

DIPLOMARBEIT

Titel der Diplomarbeit

Investigating the role of MyD88 adaptor-like (Mal)/TIRAP in functional recovery and neuronal survival following sterile peripheral facial nerve injury in mice.

Verfasserin

Marion Nidetzky

angestrebter akademischer Grad

Magistra der Naturwissenschaften (Mag.rer.nat.)

Wien, 2012

Studienkennzahl lt. Studienblatt:	A 490
Studienrichtung lt. Studienblatt:	Diplomstudium Molekulare Biologie
Betreuerin	Univ.Doz. Dr. Monika Bradl

Contents

Abstract

In most neuropathological conditions, robust activation of brain innate immunity occurs. Central nervous system (CNS) innate immune response is characterised by the engagement of the two arms of innate immunity (Complement System and Toll-like receptors, TLRs) and by the activation of neurons, microglia and astrocytes, resulting in rapid production of inflammatory cytokines and chemokines via activation of signal transduction pathways, i.e., NF-κB.

In this thesis we studied the possible role of MyD88 adaptor-like (Mal)/TIRAP in functional recovery and neuronal survival following sterile peripheral facial nerve axotomy and nerve crush in wild type (WT) and Mal knock out (KO)-mice. Peripheral facial nerve injury leads to a total paralysis of whiskers and functional recovery of whisker movement following injury occurs over time. Recovery of whisker vibration and whisker movement was monitored for 31 days post axotomy. We have demonstrated that during the first 14 days post lesion the functional regeneration of the facial nerve was similar in axotomised WT- and MalKO-mice, except for a slight onset delay in MalKO-mice. In WT-mice ongoing functional recovery of whisker movement and vibration was observed, while MalKO-mice show growing impairment after day 14.

Cell counts after 31 days show a significantly higher motoneuron survival in WT-mice (60,1%) compared to MalKO-mice (50,4%). Additionally we determined relative protein levels of GFAP, SHP-1, IRAK-1 and CD11-b. Relative GFAP levels are distinctly elevated in MalKO mice compared to WT mice while relative Shp-1 levels are reduced as well as relative IRAK-1 levels, suggesting an increased inflammatory response in MalKO-mice following peripheral injury. These results suggest that innate immune mechanisms associated to Mal/TIRAP signalling play a role in regulation of motoneuron survival and therefore also functional recovery following sterile facial peripheral nerve injury.

Zusammenfassung

Die meisten neuropathologischen Krankheiten lösen eine ausgeprägte Aktivierung des angeborenen Immunsystems im Gehirn aus. Diese ist einerseits durch Beteiligung der zwei Hauptbereiche des angeborenen Immunsystems charakterisiert (Komplement System und Toll-like Rezeptoren) und andereseits durch die Aktivierung von Neuronen, Mikroglia und Astrozyten, welche über Signalwege, wie zum Beispiel den NF-κB-Weg, in rapider Produktion von entzündungsauslösenden Cytokinen und Chemokinen resultiert.

In diesem Projekt wurde untersucht welche Bedeutung MyD88 adapter-like(Mal)/ TIRAP im Kontex von funktioneller Regeneration und dem Überleben der betroffenen Neuronon nach steriler, peripherer Gesichtsnervaxotomie und Gesichtsnervquetschung in WT- und KO-Mäusen zukommt. Diese Verletzungen führen zu totaler Paralyse der Schnurrhaare, mit funktionaler Regeneration die während der darauffolgenen Wochen stattfindet. Die Regeneration von Vibration und Bewegung der Schnurrhaare wurde für einen Zeitraum von 31 Tagen überwacht. Wie wir zeigen konnten, verlief die Heilung der Schnurrhaarbewegung und -vibration in WT- und MalKO-Mäusen während der ersten Periode von 14 Tagen parallel, zu Anfang mit minimaler Verzögerung in MalKO-Mäusen. Daran anschließend setzte sich in WT-Mäusen die Regeneration relativ stetig fort, während in MalKO-Mäusen wachsende Verschlechterung beider Parameter zu beobachten war. Dazu passend wurde 31 Tage nach Axotomie eine signifikante Differenz in der Zahl der überlebenden Neuronen zwischen WT-Mäusen (60,1%) und MalKO-Mäusen (50,4%) beobachtet. Zusätzlich wurden die relativen Proteinlevel von GFAP, SHP-1, IRAK-1 und CD11-b festgestellt. Die relativen Proteinlevel von GFAP war in MalKO-Mäusen im Vergleich zum WT deutlich erhöht während sie für SHP-1 ebenso wie für IRAK-1 reduziert waren, was auf eine erhöhte Entzündungsantwort in MalKO-Mäusen hindeutet. Diese Ergebnisse geben Anhaltspunkte dafür, dass angeborene Immunmechanismen in Verbindung mit Mal/ TIRAP Signalwegen eine nicht zu unterschätzende Rolle in der Regulation von Motorneuronen-Überleben und damit funktioneller Regeneration nach einer sterilen Gesichtsnervenverletzung in der Peripherie spielen.

1 Introduction

Innate immunity is the first line of sensors for and defence against environmental pathogens and also an important regulator of the adaptive immune system. Toll like receptors (TLRs, pattern recognition receptors) and complement system are the two pillars of the innate immune response against pathogens.

1.1 TLR

TLRs are trans-membrane receptors that contain leucine rich repeats (LRR) in the ectodomain, a trans-membrane domain and a Toll-IL-1R (TIR) domain on the intracellular part, representing an essential part for signal transduction [1] in innate immune responses. Activation of TLRs hence induces a tightly controlled signalling cascade which - overstimulated - can lead to severe inflammatory auto immune diseases [2]. TLRs are highly conserved and get activated mainly by specific mutation resistant molecular patterns found in pathogens so called pathogen-associated molecular patterns (PAMPs) [3, 4].

TLRs can be activated by various stimuli, nearly all of them pathogen associated molecular patterns (PAMPs), like LPS or RNA and others molecules found on the surface or in debris of pathogens [3]. This can lead to the induction of several different transcription factors like interferon regulatory factors (IRFs), activating protein-1 (AP-1) and nuclear factor-κB (NFκB), which in turn modulate specific immune responses.

1.1.1 Types and occurrence of TLRs

To date there are 13 different TLRs that have been identified. TLR-1 and TLR-2 are known to form heterodimers and detect bacterial triacylated lipopeptides, however, if building a heterodimer with TLR-6, TLR-2 recognises bacterial diacylated lipopeptides. One of the strongest known triggers for the innate immune system – LPS – is identified by TLR-4, building a homodimer as well as TLR-9 which detects unmethylated CpG containing DNA-motifs of bacteria and viruses. TLR-3 – binding viral double-stranded RNA (dsRNA) - and TLR-5, which senses flagellin from bacteria, are also thought to build homodimers. Single stranded (ss) viral RNA is bound by TLR-8 that has been shown to dimerise with TLR-7 and 9 and to antagonise signalling by TLR-7 or TLR-9 [5]. TLR-10 has shown to be able to homodimerise but also to build heterodimers with TLR-1 and TLR-2 [6]. TLR-11 recognises profilin of protozoan parasites [7] but have also been shown to react on uropathogenic bacteria [8, 9]. Ligands for TLR-10, TLR-12 and TLR-13 still remain to be identified.

TLRs are known to be expressed in a wide variety of cells including cells of the immune systems like microglial cells in the brain as well as astrocytes, epithelial cells and also endothelial cells [4]. Thus, it has been shown, that in different cell types different responses are triggered via different signalling pathways by the same type of TLR.

1.1.2 Signalling pathways and results of TLR activation / adaptors / mechanisms

TLRs are thought to occur in low affinity complexes where the dimers are loosely pre-assembled but not yet tightly bound. Conformational changes necessary to create a TIR-TIR-interface on the cytosolic surface takes place after ligand binding. Evidence suggests that TLRs get in closer proximity after ligand binding and create a platform for the signalling complex to be built, although the crystal structure as evidence for this platform remains to be elucidated [2].

TLR Adaptors

The next level in signal transduction is represented by the TLRs associated adaptor proteins. Five different adaptors have been identified so far: myeloid differentiation factor – 88 (MyD88), MyD88 adaptor-like protein (MAL) also known as Toll-IL-1 Receptor adaptor protein (TIRAP), TIR domain containing adaptor protein inducing IFNβ (TRIF), TRIF related adaptor molecule (TRAM) and sterile alpha and armadillo-motif-containing protein (SARM).

MAL / TIRAP MAL was found to be one of the essential factors for an early immune response in several different infections [10-13]. One of its major characteristics is its electro-negativity. Most of the TLRs are electronegative and bind well with MyD88, being electro-positive. TLR2 and TLR4 though, need the electronegative MAL as a bridging adaptor as themselves are largely electro positive and therefore not able to bind MyD88 directly [14, 15]. Its PIP-2 (phosphatidylinositol-4,5-bisphosphate) binding site on the N-terminus recruits MAL to the plasma membrane in the direct vicinity to TLR2 and TLR4 [16]. Absence of MAL or MyD88 leads to massively impaired immune responses upon stimulation of TLR 2 and 4 *in vivo* and *in vitro*. TNF-production is abolished and only a delayed induction of NFκB takes place [2]. Tyrosin phosphorylation of MAL also renders it subject to degradation mediated by SOCS1 (Suppressor of cytokine signalling 1)[17]. This represents a highly important regulation against hyperactivation through LPS, as demonstrated in SOCS1 deficient cells [17, 18], MalKO-cells show no activation of NFκB or p38 via the TLR2 pathway. They also exhibit only a delayed NFκB activation via the MyD88 independent signal transduction of TLR4 via TRIF [19, 20].

Caspase-1 cleaves a C-terminal part of MAL, a modification essential for its function. This was shown by the addition of caspase-1 inhibitor ZVAD-Cmk inhibiting NFκB activation by LPS and therefore abolishing a major pro-inflammatory pathway. Phosphorylation of p38 in response to Pam3Cys linking caspase-1 activity was also shown to be abolished [22]. Phosphorylation of MAL via the tyrosines (tyr) 86, 106, 159 [23, 24] or according to [25] phosphorylation of tyr 86, 106 and 187 leads to its activation. Mutations in those tyrosines cause decreased ability to induce p-38

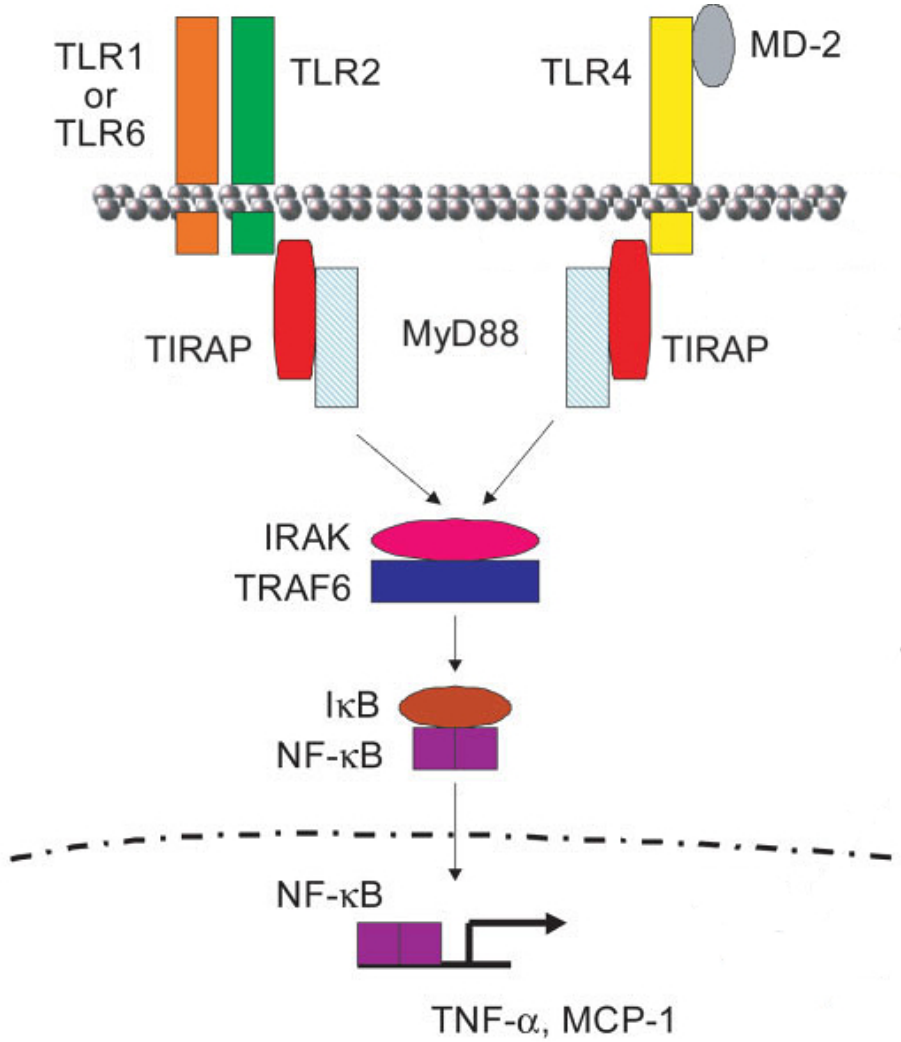

Figure 1: Activation of NF-κB via TLR2 and TLR4. Mal (TIRAP) acts as a bridging adaptor for MyD88. Subsequently activated NF-κB becomes active and enters the nucleus and induces several target genes. (Figure adapted from [21])

phosphorylation, IκBα degradation and NFκB activation upon activation by LPS. It has been shown that MAL with tyr86 and tyr187 substituted by phenylalanine, acts as a dominant negative inhibitor of LPS signalling [23, 24]. MAL also seems to play an important role in LPS-tolerance, as studies have shown decreased MAL Protein levels in the restimulation of LPS-tolerised cells.

The importance of MAL has also been shown in the MAL S180L polymorphism. This polymorphism has shown to be protective against Malaria, Tubercolosis (TB), Bacteremia and IPD (invasive pneumococcal disease) in heterozygous form. It appears to prevent the harmful over production of inflammatory cytokines by atten-

uating NFκB activation but inducing signalling sufficiently strong for host defence [26]. When reintroduced in MalKO cells, the MAL S180L polymorphism shows no activation of NFκB and, supporting those results was shown to prevent binding between MAL and activated TLR2. Another key player involved in signalling via TLR2 and TLR4 / MAL has been discovered to be Brutons tyrosine kinase (Btk). LPS induces tyrosine phosphorylation of Btk (a member of the Tec family) leading to activation of its kinase activity. Btk then phosphorylates and activates MAL. Furthermore, Btk has been shown to interact with the TIR domains of the TLRs 4,6,8 and 9 and associate with IRAK-1 (MyD88, MAL and IL-1 receptor associated kinase 1) [27, 28]. Thus X-linked agammaglobulinaemia monocytes presenting a mutation of Btk are unresponsive to LPS. It is also likely to be a main upstream target in regulation during LPS-tolerance.

IRAK-1 as well as IRAK-4 also belong to the group of proteins, modifying MAL. Experiments have shown degradation of MAL in co-expression with either of them. Furthermore the knock down of IRAK-1 and IRAK-4 or in the presence of IRAK-1 and IRAK-4 inhibitors LPS dependent MAL ubiquitination and degradation is inhibited. This seems to be responsible for a negative feedback loop in TLR2 and TLR4 signalling as well [29].

Another characteristics of MAL is its tumor necrosis factor receptor-associated factor 6 (Traf6) binding site. Reconstituting a TRAF6- binding site mutated form of MAL in MAL deficient murine macrophages shows the importance of this binding site as it doesn't restore a pro-inflammatory immune response to TLR2 and TLR4 activation. Although MAL and TRAF6 interact directly, membrane localisation is not necessary [30]. Interaction between MAL and TRAF6 leads to serine-phosphorylation of the p65 subunit of NFκB, controlling transcriptional activation but not nuclear translocation. MAL also facilitates direct recruitment of TRAF6 to the plasma-membrane in vicinity of TLR2 and TLR4 to induce a subsequent pro-inflammatory response via NFκB activation [30].

From all above described it seems that MAL plays a fundamental role in the signalling pathways following TLR2 and TLR4 activation. Signalling through TLR2 and TLR4 have been shown to be important not only during bacterial infections but

also in neuro-inflammatory processes in the CNS and this is what we intended to demonstrate in this work.

1.2 Glial cells

For a long time glial cells were considered to provide only maintenance functions to the key players of nervous tissue, i.e. neurons. The so called *nerve glue* was thought to be responsible for transporting nutrients to and waste from the neurons and provide stability for the structure of the neuronal networks. This view has changed fundamentally over the last decades and glial cells have been demonstrated to play a fundamental role in synaptic activity and neuronal plasticity by supporting neuronal and synaptic function in the central nervous system [31, 32]. They also play a role in the preservation of the host tissue integrity following injury [33] and in the CNS immune response and following peripheral and central nerve degeneration and regeneration [34] as well as learning and memory and neuronal plasticity.

1.2.1 Types

Glial cells are divided in three different main categories, astrocytes, oligodendrocytes and microglia. Each carrying out distinct functions in the complex network of the nervous system.

Oligodendrocytes

Oligodendrocytes form myelin, a lipid rich membrane, tightly and in several layers wrapped around axons to facilitate saltatory action potential propagation by electrical insulation. Action potentials *jump* from one Node of Ranvier (the small exposed space between two wraps, where ion-channels are found in high density) to the next, therefore ensuring faster signal transmission. One oligodendrocyte can wrap up to 50 axonal segments on surrounding neurons [35]. Various conditions, especially auto-immune diseases like multiple sclerosis have clearly shown how crucial the function of oligodendrocytes in signal transmission is.

Astrocytes

Astrocytes were traditionally thought to be only support for the neurons and known to regulate ion concentrations in the synaptic environment. They were also shown to provide for metabolic needs of neurons during synaptic transmission by ensheathing the neuronal synapses and regulating concentrations of ions and neurotransmitters in the synaptic cleft [36 or 37, 38]. However the knowledge about the role of astrocytes has massively changed during the last two decades. Cells classified as astrocytes are in fact a group of celltypes with specific phenotypical and biochemical characteristics. In principle all have a stellate morphology while the processes grow radially in all directions, spreading over a domain of around 200 μm diameter [39]. They represent more than 50% of cells in the CNS and are organised in glial networks. Long distance communication takes place via gap junctions established between adjacent processes of two astrocytes [40]. Probably the broadest distinction to make is the difference between protoplasmic astrocytes in the grey matter which are ensheathing synapses and fibrous astrocytes in the white matter, insulating the nodes of Ranvier. However, there exist also highly specialised types of astrocytes such as Bergmann glia in the cerebellum and Muller glia of the retina [41]. Muller glia show characteristics of immature astrocytes as they express vimentin [42]. Additionally the cell membranes of astrocytes exhibit a great variety of specialisation, dependent on the area or contact site they are in. For example in close proximity to the synaptic cleft various kinds of ligand- or voltage-gated ion channels and transporters [43] can be found in the astrocytic membrane.

Astrocytes interact with neurons, microglia and blood vessels and communicate mostly via neurotransmitters but also via gap junctions [39]. Generally resting astrocytes are star shaped cells with long processes growing out in all directions [40]. Thus astrocytes have been shown *in vivo* and *in vitro* to respond via calcium signalling to a great variety of physiological and pathological stimuli [39].

Activation of Astrocytes Activated astrocytes play a major role following nervous tissue injury, CNS trauma and in a number of neuroimmunological and neuroinflammatory conditions. Astrocyte activation in response to injury takes place in several

gradual stages and is highly dependent on timing, characteristics and severity of the injury. In the early stages of activation, astrocytic morphology and GFAP expression changes, depending on and regulated by neuronal activity [42]. In later stages astrocytes show increased levels of GFAP and Chemokines, and increased protein levels of TLRs. Also gradually, dependent on duration and severity of the stimulus, a set of different pro and anti-inflammatory cytokines is secreted by these cells [42, 44].

Following neuronal injury activated astrocytes can withdraw their protrusions from a neuron which brings them one step further towards cell death. At the same time release of neurotrophic factors by astrocytes can facilitate regeneration and repair. However, it can also lead to glial scar formation within the CNS, which, in turn, can impair nervous outgrowth and full reinnervation and regeneration [45]. Thus, it seems likely, that activation of astrocytes and the active involvement of the astrocytic network can have both, positive and negative outcomes, depending on circumstances and triggers involved. Also the ability to move molecules between extracellular and intracellular space renders them an important player in all kinds of CNS and nerve injury. Astrocytes are likely to determine the tissue response and partly the amount of tissue damage [46]. Glutamate, although being a neurotransmitter is toxic at elevated concentrations. Transporters present in the astrocytes membrane uptake glutamate from the extracellular space and help therefore preventing excitotoxic damage. They also buffer K+, and deal with free radicals - these are some of the neuroprotective astrocytic functions [47]. Neurons and glia can release pathological amounts of glutamate in case of traumatic injury or ischemia [48]. However, the protecting function of astrocytes can be reduced in an so called Excitatory Crisis and in the worst case will be reversed, resulting in elevated damage to the neuronal network [49]. Again, activated astrocytes are active in both, protective and damaging processes.

Microglia

Microglia are cells of the immune system and developmentally derived from bone marrow precursor cells. Representing about 10-20% of all glial cells, microglia are

considered to be the macrophages of the brain. At rest they constantly extend and retract highly motile processes covering a 30 to 50 μm wide area in order to keep the parenchyma under tight surveillance and scan for any sign of tissue damage. Microglia are considered to build the first line of defence against injury in the brain and get activated by any abnormal substances like lipopolysaccharide (LPS), proinflammatory cytokines or cell necrosis factors [50]. Moreover neurons can also modulate the activation status of microglia via neurotransmitters or neuromodulators [51].

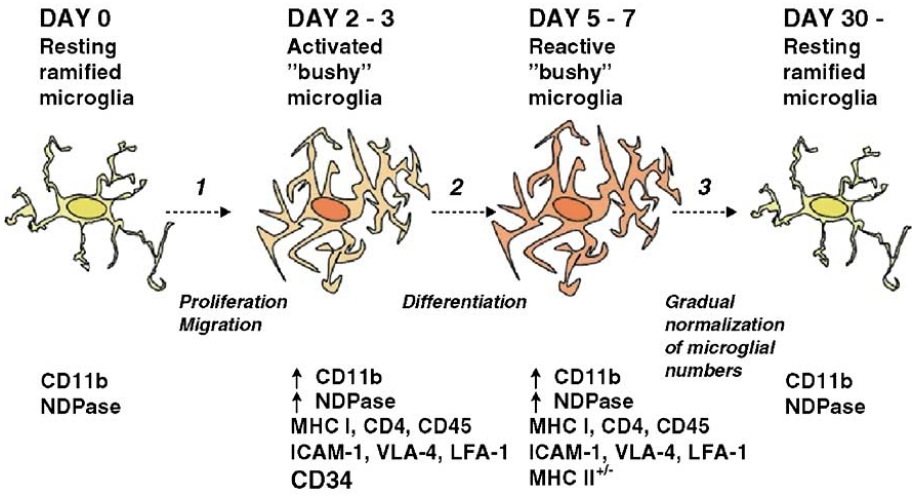

Figure 2: Schematic view of the stages of microglial activation. [81]

Activation of microglia Microglial activation - as is the case for astrocytes is characterised by phenotypical biochemical, structural and functional changes in a multi-stage process. Once activated, microglia loose their ramified morphology. The rather small cell body becomes noticeably thicker and the protrusions shorten and thicken, giving the microglial cell an amoeboid shape in which cells become motile Fig. **??** . Microglial cells then start to express cell surface proteins typical for antigen-presenting cells (APCs) like T- and B-lymphocyte markers, immune cell antigens and major histocompatibility complex (MHC) antigen. At the same time a massive proliferation takes place, to elevate the rather low numbers of microglial cells in place to accomplish their neuroimmune functions [51]. Microglia then start to migrate towards the lesion. Included in the changes occurring during activation, microglia also gain the ability of phagocytosis, and secrete proinflammatory

cytokines leading to more activated cells, but also start removing the activating antigen, engulfing debris that could lead to further inflammation and tissue injury. This helps to prevent enhancement of inflammation. Once activated they are also capable of producing N-methyl-D-aspartate (NMDA) receptor agonists [52] as well as free oxygen radicals [53] and nitric oxide [54] all being potentially neurotoxic. However, microglia also secrete growth factors like transforming growth factor-β1 (TGF-β1) [55], facilitating tissue regeneration and damage repair.

1.2.2 Glial activation and communication between microglia and astrocytes

Microglial and astrocytic activation are linked very closely although occurring at different time-points. In comparison, microglia are activating earlier and are more sensitive than astrocytes as it has been shown for experimental autoimmune encephalomyelitis (EAE) [56] and Alzheimer's disease [57]. In a model for neurodegeneration, (the administration of Trimethyltin (TMT) a chemical causing massive neuronal death already at a low dose) Microglial response was already measured in non-neurotoxic conditions [51] while astrocytic activation (with GFAP as indicator for astrocytic activation) was observed to take place at a later time compared to microglial activation [58]. This shows evidence for microglial cells responding more sensitive and also earlier than astrocytes.

Astrocytes - once activated - in turn activate distant microglia and alter the microglial response [51]. Distant activation was originally thought to take place only by calcium waves propagating along astrocytic networks. Later, adenosine triphosphate (ATP) was found to be another key player in the signal transmission. Microglia have been observed to express purinic receptors and getting activated by ATP [51].

Besides all these damage exacerbation, astrocytes have been found to have an inhibitory effect in their communication with microglia. They help preventing damage by inhibiting NO, reactive oxygen species (ROS) and TNF-α secretion [51]. In addition TGF-β has been found to be the responsible factor for deactivating mi-

croglia and attenuating chemotactic migration towards the injured site [59]. TGF-β reverses a lot of modifications occurring during microglial activation. It also leads to down-regulation of surface molecules responsible for antigen presentation and secretion of proinflammatory cytokines and radicals [60, 61]. Additionally the activation of NF-κB and the following upregulation of IL-1 mRNA levels was shown to be reduced by pretreatment of microglial cell cultures with TGF-β [51].

1.2.3 TLRs in glial inflammation

TLRs as a family of pattern recognition receptors are well known to play a major role in CNS innate immune responses to infectious diseases. Recent data also indicate participation of TLRs in tissue injury, neurodegeneration and autoimmunity. Glial cells express several types of TLRs, particularly when activated but evidence can also be found for TLR2 and TLR4 to be expressed constitutive in different brain areas. TLRs 2 and 4, which are both interacting with MAL during signal activation, are relevant for this thesis and are both expressed on microglia as well as on astrocytes. Even microglial apoptosis in an TLR2-dependent manner was shown to occur, likely to prevent bystander damage [21, 49]. Their functional significance in astrocytes remains subject to further studies.

1.3 Post-lesional plasticity – Nerve regeneration

1.3.1 The rodent facial nerve axotomy model

The rodent facial nerve axotomy model is one of the most used and best known and studied models for nervous injury and following degeneration and regeneration of the nucleus as well as functional recovery *in vivo*. This particular model provides several advantages. First and foremost it provides a paired experimental system with a direct control in the contralateral facial nerve and facial nucleus. The surgical procedure is comparably easy and is only of mild severity. The chance of contamination of the nucleus by blood is very low as no breach of the blood brain barrier happens. Also the site of the injury is far enough away from the actual nucleus and no CNS

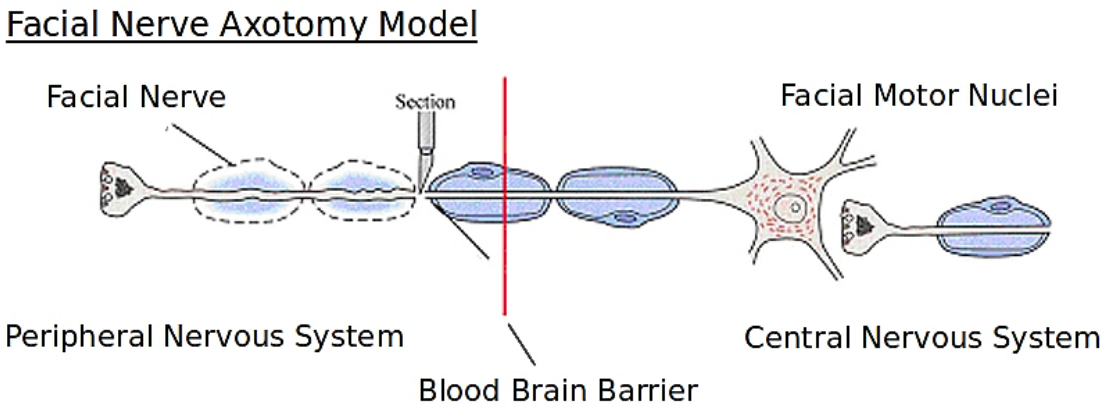

Figure 3: Schematic view of a classical motoneuron with cell body in the CNS and axonal endplate in the periphery [with friendly permission of Dr. A. Campos-Torres].

trauma takes place [62, 63]. Representing several different experimental systems in one, this system also is well studied in terms of different severities of lesions like nerve avulsion, nerve transsection and nerve crush. Depending on severity of the lesion and distance of the lesion to the cell nucleus, neuronal cell death is more or less likely to take place [64]. Major differences have shown between different species. For example in mice a significant infiltration of the facial nucleus with activated T-lymphocytes takes place in the later stages (around 14 to 30 days) of neuronal cell death. Activated microglial cells are thought to act as antigen presenting cells in this process. They are starting phagocytosis and expressing a high levels of major histocompatibility complex (MHC) class I and II molecules [65].

Anatomy of the facial nerve model

The facial nerve is the 7^{th} of 12 paired cranial nerves. In all mammals the motor branch controls the muscles of facial expression and functions. Its sensitive branch plays a role in taste sensations of the anterior two thirds of the tongue. The facial nucleus is located in the furthest ventral part of the posterior pons and the anterior medulla in the brain stem. The facial nerve leaves the skull at the level of the stylomastoid foramen and divides into two branches. The lower branch and part of the upper branch innervates the vibrissae follicular muscles. The second part of the upper branch leads up to the eye and is responsible for the nictitating reflex [66, 67]. The facial nucleus is divided in several sub-nuclei, reaching into the above

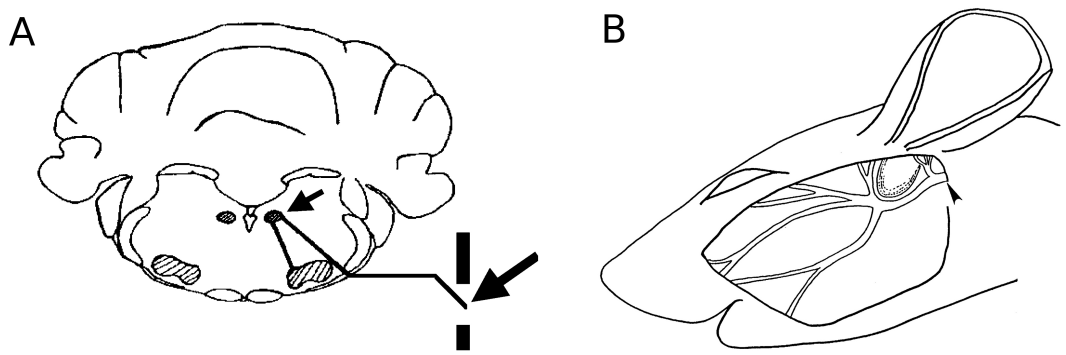

Figure 4: Anatomy of the facial nerve model. (A) Facial nuclei (hatched areas) located furthest ventral in the posterior pons. Facial nerve trajectors around the nucleus abducens indicated by the small arrow and leaves the skull at the levels of the stylomastoid foramen. The facial nerve is cut 2 mm after (big arrow). (B) Schematic drawing of the facial nerve depicting the branching out into an upper part and a lower part. The place of the axotomy is indicated by the black arrow [A: adapted from [65], B: adapted from [67].

described different branches of the facial nerve. However, motoneurons themselves are considered to be very heterogenous in terms of size and shape, although the arrangement mirrors the innervation in the whiskers, with the neurons innervating rostral whisker muscles are found laterally while the ones, representing the caudal whisker muscles are located medially in the facial nucleus [68].

Regeneration in the rodent facial nerve axotomy model

Peripheral nerve axotomy was shown to elicit a strong tissue response of the microenvironment of the corresponding area in the CNS as well as in the affected nerve cell bodies. Consistent with those findings, energy turnover and enzymatic activity in the involved neurons increases. However, axonal reactions appear to be completely independent from retrograde transport in the injured motor neuron. Microglial cells and astrocytes become activated and - together with the affected neurons - start a well organised regeneration programme. This involves increasing expression of adhesion molecules with simultaneously reducing functions and protein expression involved in classical neuronal transmission.

Other changes taking place during regeneration are so called “synaptic stripping” and loss of synaptic boutons. This is followed by sheet like lamellar extensions of astrocyte processes which cover all the areas of bouton loss. Astrocytes seem to play

a major role in protecting the regenerating neuron from phagocytosis by microglia [65]. Microglia also seem to play a protective role by secreting glutamate, helping to maintain glutamate homoeostasis [65].

In order to allow neurite outgrowth debris derived from the axotomised part of the axon has to be removed. It takes about 4 weeks post transection for re-innervation of the target musculature. Several neurotrophic and growth factors like Brain-Derived Neurotrophic Factor (BDNF) and Nerve Growth Factor (NGF) have been shown to play an essential role in the regeneration process, although recovery of function seems to be barely affected by these growth factors and has been found to be limited or even unchanged [65].

Loss of motor neurons in the peripheral facial nerve axotomy seems to be species dependent and ranges at up to 50% in mice while in rats depending on strains about 80% of motor neurons survive the procedure.

1.4 Aim of the project: Investigating the role of MAL in Facial motor neuron survival and functional facial nerve recovery in response to peripheral nerve injury

The aim of the project for this thesis was to study the role of MAL/TIRAP signalling after nervous injury. This included the impact on glial activation following peripheral facial nerve axotomy. Additionally the influence of MAL/TIRAP on facial motor neuron survival after the lesion and functional recovery of whisker movement following peripheral facial nerve axotomy within a window of 31 days was under investigation to get a more comprehensive picture.

2 Material and Methods

2.1 Material

2.1.1 Genotyping

- RNA extraction kit: RNeasy FFPE Kit (50) [Quiagen]
- reverse transcription (RT):
  - polymerase: M-MLV Reverse Transcriptase, 50000 u, 200 u/μl [Promega]
  - M-MLV RT 5x Buffer M531A, 23713920, [Promega]
  - RNasin RNase Inhibitor, 10000 u, 40 u/μl [Promega]
  - Deoxynucleotide Solution Mix #N0447L, 10 mM each dNTP [Biolabs]
- polymerase chain reaction (PCR):
  - Primers:
    - MAL A: 5'-CATCCTGTGTGGCTGTCTGTGAACCAT-3'
    - MAL B: 5'-TGGCCAATGTGTGAGCAAGTTCTGTGC-3'
    - MAL C: 5'-ATCGCCTTCTATCGCCTTCTTGACGAG-3'
  - HotMasterMix(2,5x) [Eppendorf]
  - Thermo Cycler: Light Cycler [Roche]
- agarose gel:
  - agarose: [FISHER]
  - 1x TAE: 40 mM Tris acetate, 1 mM EDTA (ethylenediamine tetraacetic acid, pH 8.0

- marker: Gene Ruler (TM) Ultra Low Range DNA Ladder, 0,1μg/μl, [Fermentas]
- ethidiumbromide: [Sigma, Aldrich]
- running buffer: 1x TAE
- equipment: Electrophoresis DNA gel system [Promega]
- measurements/pictures: Snap Gene viewer

2.1.2 Surgical procedures

- Mice: Wild Type C57 B6 and MalKO mice were bred in the animal facility at the institute of Immunology at the National University of Ireland, Maynooth
- As the MalKO mice were bred from controlled homozygous MalKO parents only random samples were taken for genotyping. MalKO mice were also on C57B6 background.
- Anaesthesia:
  - MatrxTM Veterinary Anesthetic Gas Scavenger [Midmark]
  - Medical Oxygen [BOC Medical]
  - Filter: Active Scavenging Unit [VetTech Solutions LTD]
  - Cage for anesthesia: [VetTech Solutions LTD]
  - Anaesthetic: IsoFlo 100% w/w Inhalation Vapour, Liquid, Isoflurane 250 ml, [Abbott Laboratories Ltd]

2.1.3 30 day recovery and neuronal survival in the facial nucleus

- PBS (phosphate buffered saline, 0,1 M, pH = 7,4), [Life technologies]
- 4% solution Paraformaldehyde (PFA) [Sigma] in sterile PBS, pH 7,3
- Euthatal (Merial) Solution for injection [Merial Animal Health Ltd.], 200 mg Pentobarbital Sodium in 1 ml, diluted to final concentration of 70 mg/ml
- Xylenes, [Sigma Aldrich]

- Tissue Processor: ThermoShandon Citadel 1000, [ThermoShandon]
- Embedding Unit: Shandon Histocentre 2, [Shandon]
- Shandon Biopsy Cassettes with attached lid, [Thermo Electron Corporation]
- disposable Base Molds, [Simport]
- Menzel-Gläser SUPERFROST R Plus, Microscope Slides, [Thermo Scientific]
- Microtome: Shandon Finesse 325, [Shandon]
- Chloroform, [Fisher Chemical]
- 0,1% [w/v] Cresyl violet solution, Cresyl Violet acetate, [Sigma]
- DPX mountant for microscopy, [BDH Laboratory Supplies]
- Cryotome: ThermoShandon
- Glue: [Fisher]
- Giemsa staining, Riedl Haen
- Fatpen: [DAKO]

Immunohistochemistry

- Vibratome: Integraslice 7550MM, [Campden Instruments]
- Primary antibodies:
  - GFAP: rabbit anti GFAP, [DAKO Cytomation]
  - IRAK-1: IRAK-1 (H273) rabbit polyclonal IgG, [Santa Cruz]
- Secondary antibody:
  - Alexa Fluor 488, green, [invitrogen]
- Nuclear staining: DAPI [Roche]
- Neuro Trace, [Molecular Probes]
- Mounting Media: Aqua Poly/Mount Coverslipping Medium, [Polysciences Inc.]

Western blots

- NanoDrop 1000, [ThermoScientific]
- Odyssey Infrared Imager (Model 9120), [Li-Cor Biosciences]
- PBST (0,1% Tween)
- Tween 20, [Sigma Aldrich]
- N,N,N',N' Tetramethylenediamine (TEMED), [Sigma]
- Ultra Pure Protogel, [national diagnostics]
- 4X Laemmli Lower Tris (1,5 M Tris, 0,4% SDS, pH 8,8, with Tris Base)
- 4X Laemmli Upper Tris (0,5 M Tris, 0,4% SDS, pH 6,8, with Tris Base)
- 10X SDS Laemmli Running Buffer (0,25 M Tris, 1,92 M Glycine, 1% SDS, pH 8,3), diluted 1:10 for experiments
- Transfer Buffer (25 mM Tris Base, 0,2 M glycine, 20% methanol
- 3X Laemmli Sample Buffer (0,25 M Tris, 6% SDS, 40% glycerol, 0,04% Bromophenol Blue, 20% 2-mercaptoethanol)
- Marker: Page Ruler TM Plus, Prestained Protein Ladder, [ThermoScientific]
- Primary Antibodies:
  - CD11 b: rat anti mouse-CD11b, [eBioscience]
  - GFAP: rabbit anti GFAP, [DAKO Cytomation]
  - IRAK-1: IRAK-1 (H273) rabbit polyclonal IgG, [Santa Cruz]
  - SH-PTP1: SH-PTP1 (C-19), rabbit polyclonal IgG, [Santa Cruz]
- Secondary antibody:
  - Odyssey Goat anti-Rabbit IR Dye 800 CW, [Li-Cor Biosciences]
  - Odyssey Goat anti-Mouse IR Dye 680, [Li-Cor Biosciences]
  - Streptavidin (diluted 1:200) [Invitrogen]

Lysisbuffer

Lysisbuffer			1% IGEPAL; 0,1% SDS			
	Stock Conc.		Final Conc.		3,0 ml	
ddH2O (autoclaved)					2291,3	µl
Complete Mini, Protease inhibitor cocktail tablets [Roche]	tablets				1,0	
NaCl [Sigma]	1	M	150	mM	454,6	µl
Sodium Phosphate Mono [Aldrich]	1	M	10	mM	30,0	µl
IGEPAL CA-630 [Sigma]	100	%	1	%	30,0	µl
NaF [Sigma Aldrich]	0,5	M	50	mM	37,5	µl
Na3VO4 [Sigma]	100	mM	1	mM	30,0	µl
DTT (Dithiothreitol)	100	mM	1	mM	30,0	µl
PMSF (in EtOH) [Sigma]	100	mM	1	mM	30,0	µl
Benzamidine (in EtOH)	1	M	3	mM	9,0	µl
EDTA (Ethylene diamine tetra-acetate) [Sigma]	0,5	M	2	mM	12,0	µl
EGTA (Ethylene glycole tetra-acetate)	100	mM	1	mM	30,0	µl
N-Ethylmaleimide (in EtOH)	50	mg/ml	2	mM	15,7	µl
Na Deoxycholate [Sigma Aldrich]	10	%	0,1	%	15,0	µl
beta-Glycerophosphate disodium hydrate [Sigma]	5	mg/ml	50	mM	30,0	µl
SDS (Sodium dodecyl sulfate) [Sigma Aldrich]	10	%	0,1	%	30,0	µl

Figure 5: Ingredients for Lysisbuffer

Protein measurements

Preparation of Lysisbuffer (always prepare freshly!): Water was pipetted into a 50 ml tube and protease inhibitor tablets were dissolved. The tube was placed on ice and all the ingredients of above table added and then vortexed until the IGEPAL was completely dissolved. It was then centrifuged for 10 minutes at 3000 rpm to dissolve the foam and the pH was adjusted at 7,3 with 2M NaOH. The buffer has to be kept on ice.

2.2 Methods

2.2.1 Genotyping to guarantee homozygous MalKO in used mice

RNA-extraction

RNA-extraction was done exactly to the protocol of RNeasy FFPE Kit [Qiagen].

RT

2 μg of RNA were added into a sterile RNase-free 500 μl tube, with 1 μg random primer and water was added to a total of 13,5 μl. The tube was heated to 70°C for

5 minutes, then immediately cooled on ice and spinned briefly to collect the solution at the bottom. A mastermix was prepared consisting of M-MLV Reaction Buffer, dNTPmix (1,25 μl), 10 mM dCTP (1,25 μl), 10 mM dGTP (1,25 μl), 10 mM dTTP (1,25 μl), 25 units Recombinant RNasin® Ribonuclease Inhibitor (40 u/μl) and 200 units M-MLV RT (200 u/μl) (all this amounts are per sample). 11,5 μl of mastermix were added to each sample and mixed by gentle flicking. Tubes were incubated for 60 minutes at 37°C, then incubated for 5 minutes at 95°C and immediately put on ice. Samples were stored at -20°C until further use.

PCR

For the genotyping PCR 25 μl of Eppendorf® HotMasterMix(2,5x) were placed in a 500 μl eppendorf tube with 1,0 μl of either primer MAL A and MAL B (10 μM, each) to check for WT mice or primer MAL B and MAL C (10 μM, each) to check for MalKO mice and 23,0 μl distilled H2O and mixed. 1,0 μl of DNA was added and the PCR amplification performed in a thermal cycler with the following parameters: 1) 95°C for 5 minutes, 2) 95°C for 30 seconds, 3) 60°C for 30 seconds, 4) 72°C for 1 minute, 5) 35 cycles of step 2 - 4, 6) 72°C for 10 minutes; Both products were about 900 bp. To ensure the mouse in question is homozygous for WT or homozygous for MalKO the DNA had to be tested for both (for MalKO: no signal in WT-primers but signal for MalKO primers; for WT: signal for WT primers but no signal for MalKO primers);

Agarose gel

Agarose gel was prepared from 1,125 g agarose mixed with 75 ml 1xTAE and was dissolved by heating (microwave). 5 μl ethidiumbromide was added and the mixture poured into a small gel casting (10 cm) tray with comb and let cool down for 30 minutes. Gel was placed in a gel electrophoresis apparatus (comb at the negative end) and was submerged in running buffer (1xTAE) by a view millimetres. 5 μl ethidiumbromide was added to the positive end of the tray and 15 μl sample was loaded and run for 45 minutes. It was then viewed and photographed under UV light with an exposure time of 80 ms.

2.2.2 Surgical Procedures

Axotomy/crush facial nerve

All surgical instruments used in the surgical procedures were autoclaved and the surgical area was disinfected with alcohol (70%). WT mice (n=3) and MalKO mice (n=3) were deeply anesthetised with isoflurane, a small incision was made and the left facial nerve was exposed posterior to the left ear. The facial nerve was transsected at a point 2.0 mm inferior to the stylomastoid foramen. After suturing the skin, animals were kept on a polystyrene tray until complete recovery. Success of the facial nerve lesion was verified by observing ipsilateral whisker movement. All axotomised animals presented a complete whisker paralysis.

Unoperated WT mice (n=3) and MalKO mice (n=3) as well as sham-operated WT mice (n=3) and MalKO mice (n=3) were used as controls. Sham-operated animals that consisted of mice that were anaesthetised as described above, the left facial nerve was exposed posterior to the left ear but not cut, the skin was sutured and the animals left on a polystyrene tray for complete recovery from anaesthesia. Sham operated mice showed no signs of impairment of whisker movement and vibration. The contralateral side of the brain was used as the internal control, as the facial nerve is not anatomically connected with the contralateral side.

2.2.3 30 day recovery and neuronal survival in the facial nucleus

Monitoring of functional recovery in axotomised, nerve crushed and sham-operated mice

Following axotomy mice were examined for functional whisker movement an vibration recovery by 2 independent observers. Whisker movement and vibration was evaluated separately on a scale from 0 to 2 in 0,5 intervals. 0 representing no movement/vibration at all and 2 representing full recovery with no visible difference between the unleasionned, fully functional and lesioned side.

Perfusion and paraffination of brains

Perfusion Untreated (WT: n=3, MalKO: n = 3), sham-operated (WT: n=3, MalKO: n = 3), facial nerve axotomised (WT: n=3, MalKO: n = 3) mice were injected with a lethal doses of 150 μl Euthatal [70 mg/ml], the thoractic cavity was then opened and the animals were transcardially perfused with 10 ml sterile PBS, followed by 40 ml ice cold 4% PFA as fixative. Progress of the perfusion was monitored by the typical signs of neck stiffness and discolouring of the liver. Once the perfusion was finished, the brain was removed immediately and postfixed in 10 ml ice cold 4% PFA, stored at 4°C until used.

Paraffination Perfused brains were postfixed for 2 days in 4% PFA. They were then incubated in 70% Ethanol for about 24 h. Brains were then trimmed and put in special paraffin cassettes and transferred to an automatic tissue processor and the paraffination process was following the instructions described below:

70% Ethanol for 1h (1x), 80% Ethanol for 1h (1x), 95% Ethanol for 1h each (2x), 100% Ethanol for 1h each (3x), 1:1 Ethanol/Xylene for 1h (1x), Xylene for 1h (2x), hot Paraffin for 1h (1x);

The paraffinised brains were then collected and cast into paraffin disposable Base Molds, by using the Shandon Histocenre 2, rostral side of the brain facing up and caudal side attached to the holder.

Cutting, fixation and staining of paraffinated brain slices

Microtome sections of paraffinated brain slices Brains were installed in the microtome and trimmed. The start of the facial nucleus was histologically verified with a 10x magnification on the microscope until the 4th ventricle had changed into a diamond like shape and the cerebellar flocculus had emerged laterally. From there on 8 μm slices were cut, and transferred into cold tap water containing 25 ml Ethanol per litre. Slices were then immediately transferred to a hot water bath (42°C) to smooth out creases generated during cutting. Slices were then mounted on microscope slides and left dry at RT until used. 240 brain slices were collected per brain and stored at room temperature until used.

Fixation and staining of paraffinated brain slices Slides were incubated on a heating block for 1,5 hours at 56°C. They were then placed on preheated plastic plates and slowly cooled down for about 10' at room temperature to avoid detachment of slices during staining. Slides were then incubated in Xylene (2x 10 min) and deparaffinated over night (for at least 10 hours) in 50:50 Ethanol:Chloroform. The day after they were rehydrated in sequential baths of 100%, 95%, 70% and 50% ethanol for 5 min each. They were then rinsed shortly in distilled and sterilised water and let dry (for 3 minutes). Slides were then incubated for 5 min in 0,1% cresyl violet solution, rinsed quickly in distilled and sterilised water and differentiated in 95% ethanol for 10 min. Finally slides were dehydrated for 2x 5 min in 100% ethanol and 2x 5 min in Xylene and mounted with DPX.

Cryotome sections and Giemsa-staining of frozen brains

Cryotome sections Mouse brains which had been immediately frozen on dry ice and had been stored at -70°C are thawed slowly in the cryostat to a working temperature of -20°C. The brains were cut in half and glued to the specimen holder. 14 μm thick slices were cut with the specimen holder -19°C and working temperature -24°C, then mounted on glass slides and stored at -70°C.

Giemsa-Staining The tissue slices were dried for 30 seconds at room-temperature, circled with fatpen and incubated in 4% PFA for 15 minutes. Afterwards they were washed 3x 5 minutes in PBS and incubated for 55 seconds in Giemsa staining solution. Then the slices were washed briefly 2x in distilled sterilised water.

2.2.4 Immunohistochemistry

Vibratome sections, staining and fixation of perfused brains

Vibratome sections A WT brain and a MalKO brain perfused with PFA and incubated in PFA for 2 days were trimmed. A small piece of 2% Agarose was glued to the specimen holder with super glue and the brain was glued to the Agarose with the posterior side. The holder was filled up with PBS and slices were cut with the

following parameters: Frequency 80 Hz, advance 1 mm / second, thickness: 25 μm. A 24 well plate was prepared with 1 ml PBS per well and 3 slices per well were incubated.

Staining The slices were transferred with a brush into PBST/BSA (5%) (in a 24 well plate) and blocked for 3 h on a rocker. One set of slices was incubated in IRAK-1 antibody solution (1:500, in PBST/BSA(5%)), the second set was incubated in GFAP antibody solution (1:500, in PBST/BSA (5%)). Both were left over night at 4°C on a rocker. The next day both sets were washed three times 10 minutes in PBST on a rocker and incubated in Alexa Fluor 488 secondary antibody (1:500, in PBST/BSA(5%)) for 1 h also on a rocker. Again they were washed 3x 10 minutes in PBST. Additionally DAPI and Neurotrace staining was performed (each 1:500 in PBS) incubated for 1 h on a rocker and washed 1x 10 minutes in PBST.

Brain slices were then mounted on glass slides with Aqua Poly/mount mounting media.

2.2.5 Western blots for protein levels of GFAP, SH-PTP1, IRAK-1 and CD11b, in the facial nucleus at 2, 4 and 8 days post axotomy

Tissue collection and sample preparation

Normal control (WT: n = 3, MalKO: n =3), sham-operated (WT: n = 3, MalKO: n =3) and lesioned (WT: n = 3, MalKO: n =3) mice were sacrificed by decapitation at 2, 4 and 8 days post axotomy. The brains were removed rapidly, the facial nucleus dissected and transferred into 150 μl lysis buffer and immediately frozen in liquid nitrogen. After thawing the samples on ice, the tissue was homogenised by using a 23 G and a 27 G needle in a 1 ml syringe. The samples were again frozen in liquid nitrogen, and thawed on ice. Again the solution was homogenised with a 27 G needle and then left on a shaker for 40 minutes at 4°C. The samples were centrifuged at 13 000 rpm for 10 minutes at 4°C. The supernatant was transferred into a new Eppendorf tube and the protein concentration was measured using the

Nanodrop at 289 nm. The protein concentration of the samples was normalised by using lysis buffer. 3x sample buffer was added (to a final concentration of 1x) and they were then boiled for 5 minutes at 95°C. The samples were stored at -20°C until use.

Western Blot for GFAP, IRAK-1, Shp-1, CD11b

Western blot analysis of GFAP, IRAK-1, Shp-1 and CD11b was performed in samples of the facial nucleus, following 2, 4 and 8 days post facial nerve axotomy by conventional sodium dodecyl sulfate (SDS)-polyacrylamide gel electrophoresis according to [70]. For IRAK-1 and CD11b a 10% acrylamide gel was used, for GFAP and Shp-1 a 12% acrylamide gel. 20 μl of each sample were loaded per well. The gels were started at 90 V for 20 minutes and increased to 120 V for IRAK-1 and Shp-1 for 130 minutes, for GFAP and CD11b for 110 minutes. Following electrophoresis gels were washed for 15 minutes in transfer buffer to equilibrate them, they were then transferred onto nitrocellulose membrane (Whatman) using a semi dry blotting system at 110 mA for 110 minutes (IRAK-1, CD11b) and 100 minutes (GFAP, Shp-1). Membranes were then blocked with 5% milk/PBS for 1 hour and incubated over night on a roller at 4°C with the according antibody: rabbit anti IRAK-1 antibody (diluted 1:1000) in 5% milk/PBST, rabbit anti SH-PTP1 antibody (diluted 1:2000) in 5% milk/PBST, rabbit anti CD11b (diluted 1:2000) in 5% milk/PBST, rabbit anti GFAP antibody (diluted 1:2000) in 5% milk/PBST. The next day the blots for IRAK-1, GFAP and Shp-1 were washed 3x 15 min in PBST at room temperature on a roller and incubated for 1 h with a goat anti-rabbit secondary antibody (diluted 1,2:5000) in 5% milk/PBST on a roller at room temperature. Blots were washed 3x 15 min in PBST and 1x 30 min in PBS and scanned using the LiCor Odyssey scanner system (700 nm). Membranes for CD11b were then washed 3x 5 minutes in TBST (0,05% Tween), 1x 5 minutes in 0,1% BSA/TBST(0,05% Tween) and were incubated in streptavidin (diluted 1:200) for 1 h at room temperature. In the dark room 1,5 ml of solution A and 1,5 ml of solution B (per blot) were mixed and applied to the blot, covering it completely for about 3 minutes. The blot was placed between two layers of transparency film, in a light proof film cassette. The

two layers were sealed with tape, 2 layers of photo film were placed on top (results in less exposure of the upper film) and the cassette closed and incubated for 5 minutes. Exposed photo films were developed until the bands were visible, they were then rinsed briefly in water, and fixed for 3 minutes, then rinsed in water and left to dry. The blots were then scanned and digitalised.

3 Results

3.1 Genotyping

Genotyping was done with three primers (A, B and C), with A and B being specific for WT-mice and B and C being specific for MalKO-mice. As both products had the same size, the genotyping of each sample had to be done for both primer combinations with A and B being negative while B and C being positive to confirm homozygous MalKO-mice. Fig. **??** shows the product for WT (second lane) and the product for MalKO (third lane).

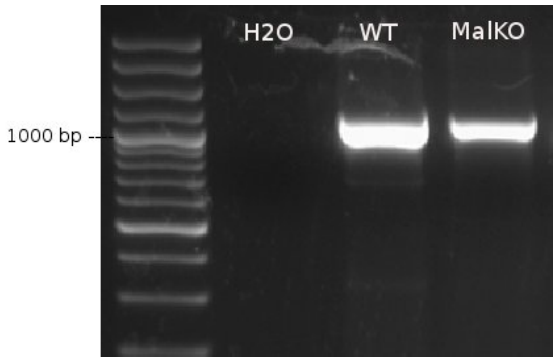

Figure 6: The product for WT as well as the product for MalKO are around 900 bp. Water was used as a control.

3.2 Recovery 31 days post axotomy

3.2.1 Functional Recovery is Impaired in MalKO mice

Observation of functional recovery of whisker vibration and movement had shown a marked difference in recovery between WT mice and MalKO mice. Whisker vibra-

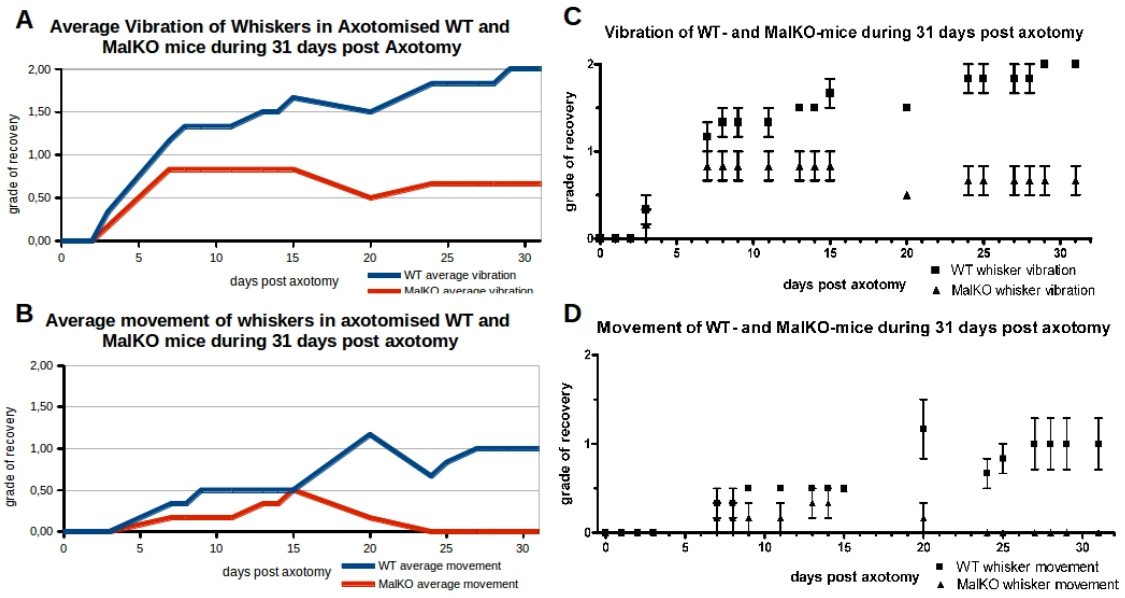

Figure 7: Recovery of vibration (A+C) and movement (B+D) (depicted as graph in A and B or dots with errorbars in C and D) of whiskers observed through 31 days post facial nerve axotomy in WT and MalKO mice. Recovery of vibration was delayed and massively impaired in MalKO compared to WT mice which made a full recovery at the end of the observation period (31 days) (A+C). Recovery of movement was only slightly delayed in the onset, only to fall back into complete paralysis from day 20 on (B+D).

tion recovery had started slightly delayed in MalKO mice and roughly parallel with the recovery of WT mice up until day 7. At that point the first stagnation in MalKO recovery (at a rating of 0,83 out of 2) became visible. From day 15 on a decrease in functionality had taken place and had stagnated at a significantly lower rate than in WT mice of 0,67 (out of 2) around day 20. WT whisker vibration recovery had slowed down but was constantly taken place up to a full recovery (rated with 2 out of 2) around day 29 (see Fig. 7A and C). Whisker movement recovery had started off equally in WT and MalKO mice and went along nearly parallel but again with a slight delay in MalKO mice up to day 15, where both had been rated at 0,5 (out of 2). From day 15 on, WT mice recovery had proceeded and stabilised at 1 (out of 2) around day 26. MalKO mice whisker movement on the other hand had declined rapidly from 0,5 (out of 2) to 0 (out of 2) from day 15 to day 24 with no further development up to the end of the observation time at day 31 (Fig. 7B and D).

Summarising whisker vibration had recovered fully in WT mice after 31 days and only to a rating of 0,5 (out of 2) in MalKO mice (see Fig. 8A). Whisker movement

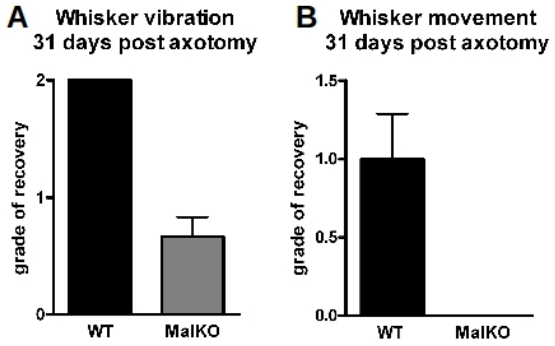

Figure 8: Recovery of vibration (A) movement (B) of whiskers at the end of the 31 days observation periode post peripheral facial nerve axotomy in WT and MalKO mice. WT mice show full recovery of whisker vibration of the injured side, compared to the contralateral side, while in MalKO the rating reaches only 0,67 (out of 2) (A). Whisker movement recovery arrives at 1 (out of 2) in WT mice on day 31, while in MalKO mice there is no movement in the ipsilateral side visible at 0 (out of 2), compared to the contralateral, uninjured side (B).

had only recovered up to 1 (out of 2) in WT mice, but had shown no lasting recovery at all in MalKO mice (0 out of 2), (see Fig. 8B)

3.2.2 Neuronal survival 31 days post axotomy

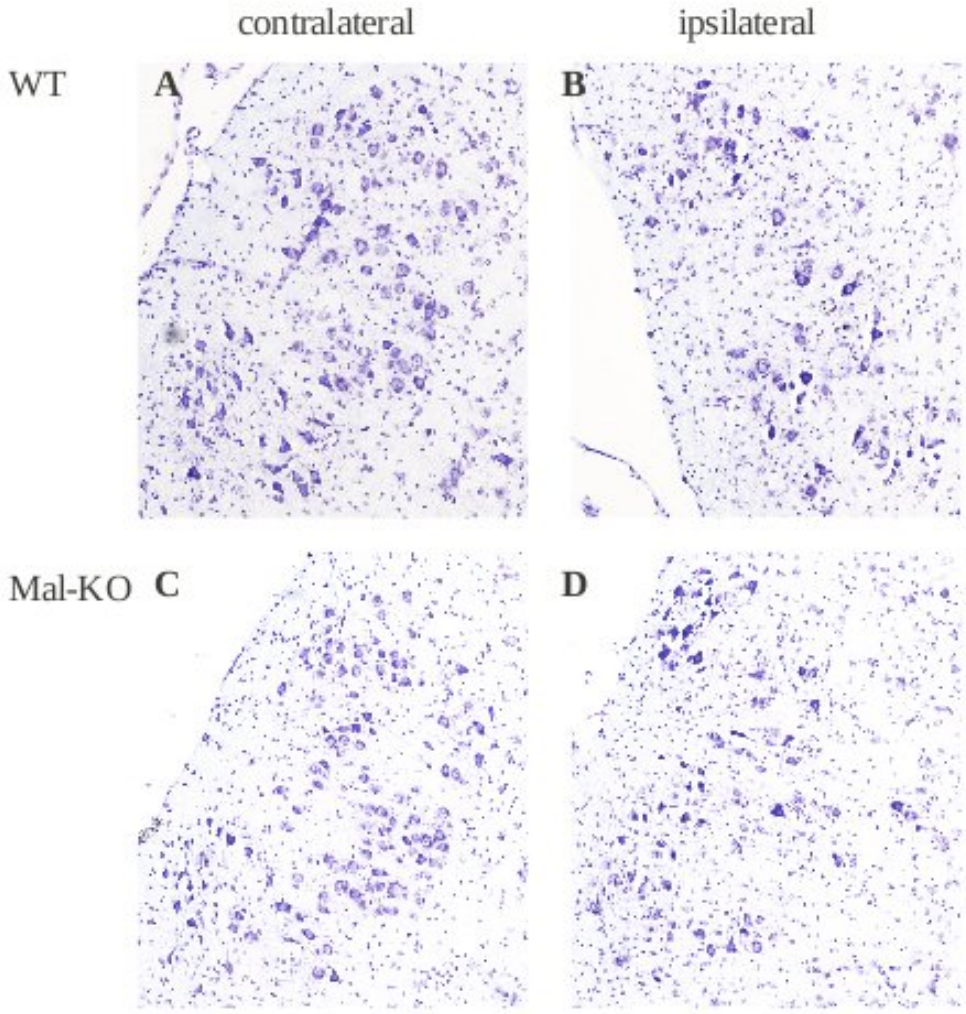

Figure 9: Facial Nucleus: Cresyl violet staining of 8 μm paraffinated coronal brainslices of WT and MalKO mice. Micrographs show the facial motor nucleus in mice with facial nerve axotomy, 31 days post operation compared to the lesioned side of the same mouse (A) WT contralateral facial nucleus; (B) WT ipsilateral facial nucleus; (C) MalKO contralateral facial nucleus; (D) MalKO contralateral facial nucleus;

Facial nerve axotomy in WT and MalKO mice led to severe motoneuron loss 31 days post lesion. Fig. 2 shows the rather dramatic loss of motoneurons in the facial nucleus. Fig. 9A shows the facial nucleus on the unlesioned side of a WT mouse while Fig. 9B represents the ipsilateral facial nucleus, where the loss of cells 31 days post facial nerve axotomy is clearly visible. Fig. 9C depicts the unlesioned side of a MalKO mouse while Fig. 9D shows the axotomised side of same mouse, again showing significant cell loss.

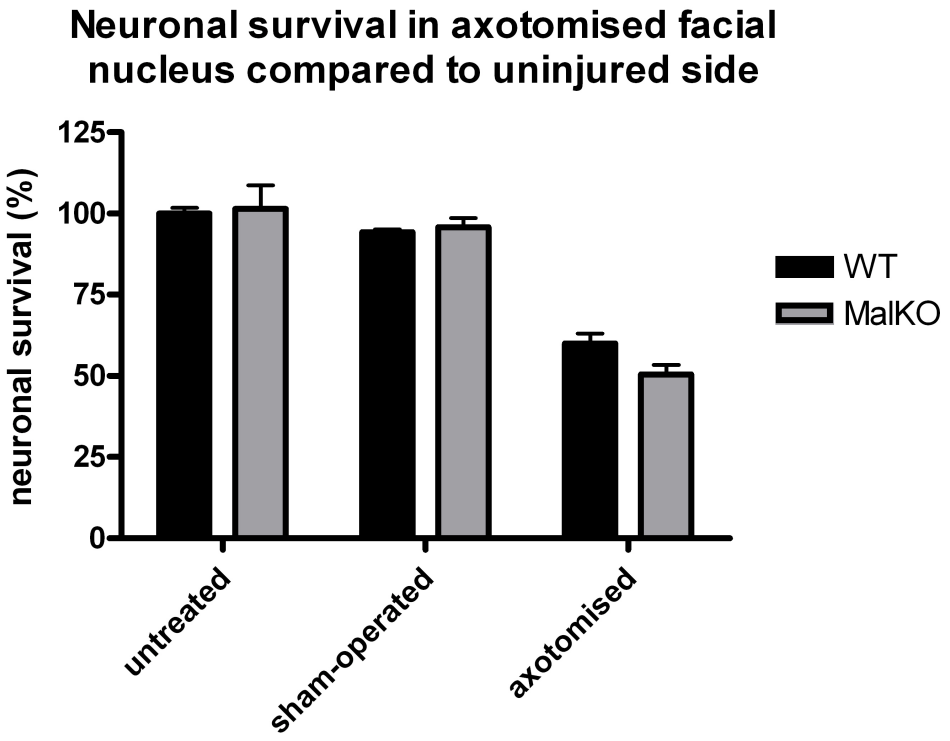

Figure 10: Neuronal survival: remaining neurons of the facial nucleus 31 days post peripheral facial nerve axotomy have been counted in the ipsilateral and contralateral nucleus. The percentage of survival was calculated compared to the unlesioned (contra lateral) side. Controls used were completely untreated mice and sham operated mice. Untreated mice and sham operated mice show no significant difference between the ipsi and contralateral side (untreated WT: 106,9% ± 8,2%, untreated MalKO: 101,8% ±13,2%; sham operated WT: 94,3% ± 1,4%, sham operated MalKO: 95,7% ± 4,9%; all mean ± SD, n=3). There is a significant difference in the neuronal survival between WT mice (60,1% ± 5,0%, mean ± SD) and MalKO mice (50,5% ± 5,1%, mean ± SD, n=3) with a P¡0,05 in one-sided unpaired t test.

As shown in Fig. 10 there is no significant difference between the ipsilateral and the contralateral side in untreated and in sham operated mice. These were used as controls for an eventual influence of the surgery itself. Motoneuron survival in axotomised mice accounts in WT for 60,1 ± 5,1% (mean ± SD, n=3), compared to MalKO mice where neuronal survival is significantly lower at 50,5 ± 5,1% (mean ± SD, n=3). The used one-sided unpaired t test shows a p value lower than 0,05. Here the lack of MAL is clearly responsible for a higher cell death in the ipsilateral facial nucleus.

3.3 Changes in GFAP, IRAK-1, Shp-1 and CD11b protein levels

3.3.1 GFAP protein level is higher in MalKO mice following facial nerve axotomy compared with WT

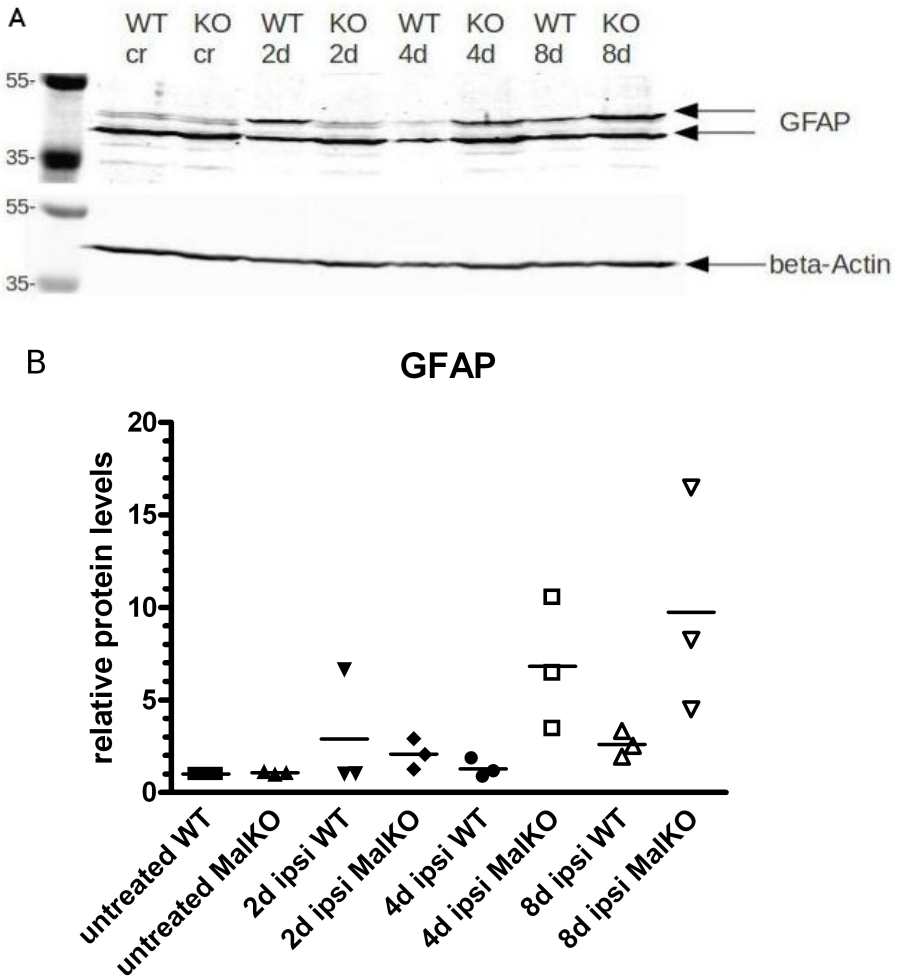

Figure 11: (A) Representative protein double band for GFAP showing clearly the increased expression in the upper band of the two signals for GFAP. (B) Figure showing relative protein levels of GFAP in the ipsilateral facial nucleus. Western blot results were normalised with beta-Actin and depicted relative to untreated WT-levels of GFAP. Clearly visible from day four on there is a trend to strongly increased levels of GFAP in MalKO mice, compared to WT.

Relative protein levels within the facial nucleus were determined for GFAP as a marker for astrocytic activation with tissue samples of the ipsilateral facial nucleus at 2, 4 and 8 days post facial nerve axotomy. Levels of GFAP increase in WT mice

post axotomy, as astrocytes get activated. When observing only the upper band of the GFAP signal (Fig. 11A), significant differences between the protein levels in WT and MalKO mice were observed, showing a stronger activation of astrocytes already at day 4 in MalKO mice, even more pronounced at day 8 (see Fig. 11B). All results were depicted relative to untreated WT-protein levels as controls.

3.3.2 IRAK-1 protein levels decrease in MalKO mice following facial nerve axotomy compared with WT

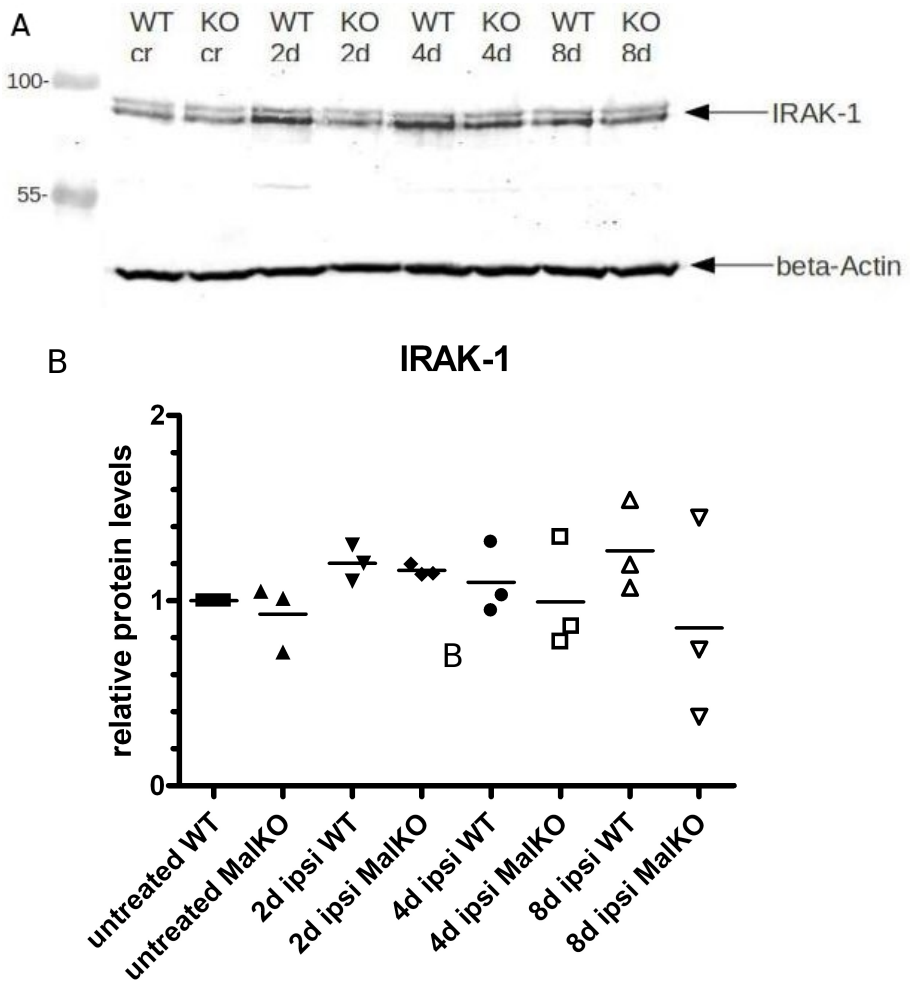

Figure 12: Relative protein levels of IRAK-1 in the facial nucleus. IRAK-1 protein levels were higher in the axotomised mice than in the controls on day 2 in both, WT and MalKO mice. While WT protein levels rise further at 4 and 8 days post axotomy, for MalKO mice protein levels a trend was observed towards a decreased amount of IRAK-1. We have observed a delayed and less important increase in the levels of IRAK-1 within the ipsilateral Facial nuclei following injury in MalKO mice related to controls.

Relative Protein levels for IRAK-1 within the facial nucleus were also observed post axotomy. Fig. 12A shows the results of the western blots, while Fig. 12B shows the relative protein levels. Although in both, WT and MalKO mice levels were slightly elevated after two days and increased further in WT mice 4 and 8 days post facial nerve axotomy, in MalKO mice an entirely different trend can be observed. After a small increase at day 2 protein levels of IRAK-1 in MalKO mice decrease below control levels at day 4 and even further at day 8.

3.3.3 Shp-1 protein levels are lower in MalKO mice following facial nerve axotomy compared with WT

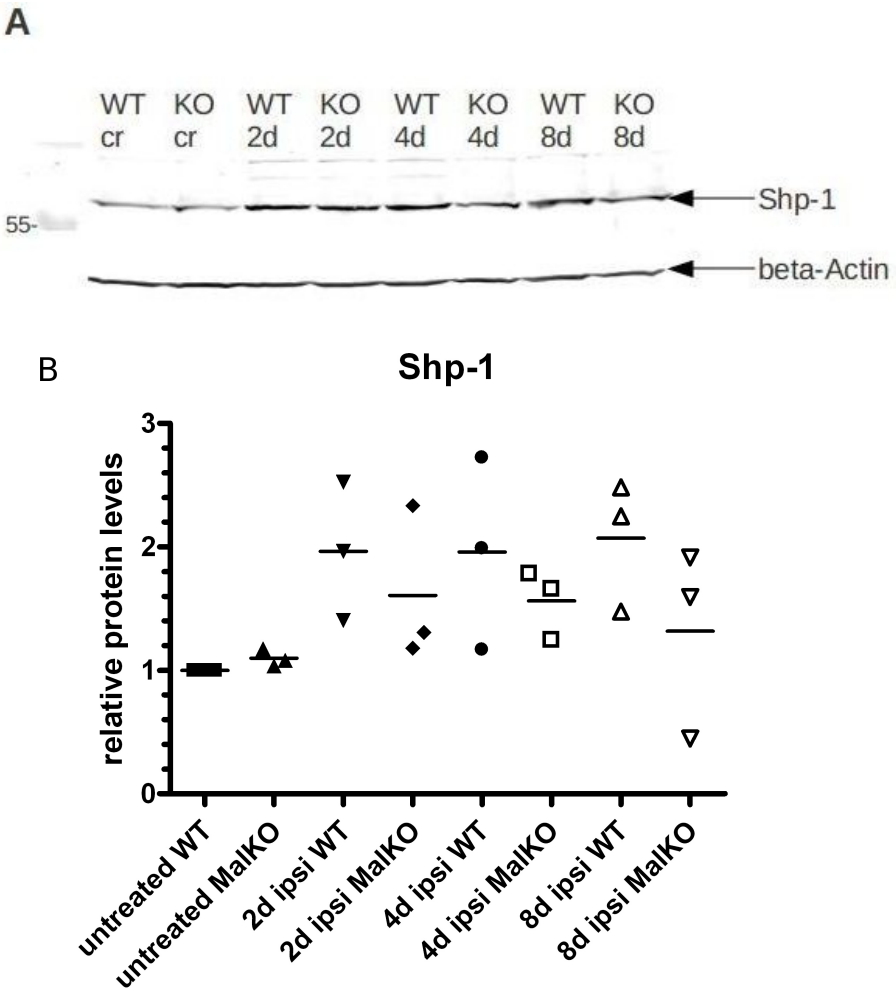

Figure 13: Analysis of relative Shp-1 levels in the ipsilateral facial nucleus relative to untreated WT levels showed as a trend slightly lower expression levels of Shp-1 in MalKO mice at 2, 4 and 8 days post axotomy. In general, relative WT levels are higher at all observed time-points. In MalKO levels of Shp-1 there is still a tendency to higher relative levels than in the untreated control group.

Shp-1 protein levels within the axotomised facial nucleus are higher than IRAK-1 with concentrations in MalKO mice being lower than in WT (Fig. 13) at all observed time-points. In MalKO mice the relative protein levels of Shp-1 are still higher than in the uninjured control group. In general both, WT and MalKO Shp-1 levels seem to peak at day 4, but this needs to be confirmed by another experiment with a bigger number of animals per group.

3.3.4 CD11b shows no specific trend following facial nerve axotomy compared with WT

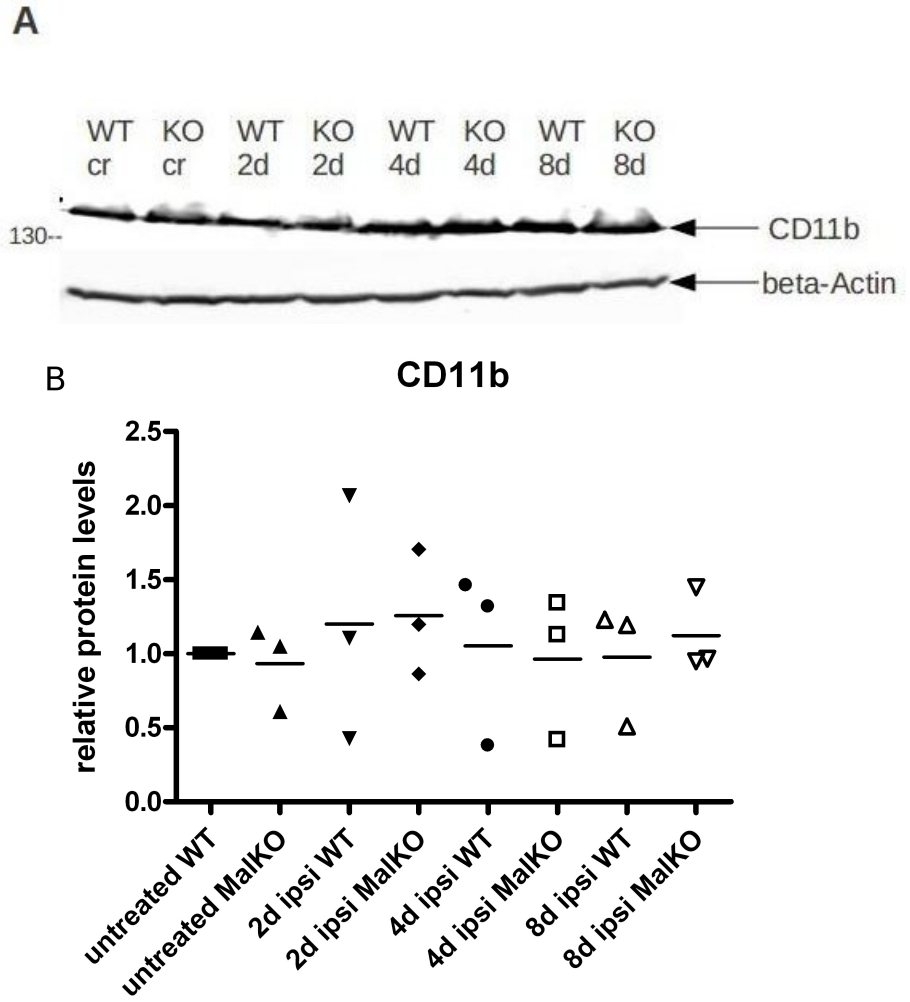

Figure 14: Relative CD11b protein levels in the facial nucleus after facial nerve axotomy. Relative protein levels of the MalKO mice are slightly lower than in the WT mice. There is no trend visible in the axotomised mice.

Relative protein levels of CD11b within the facial nucleus in axotomised mice were determined as a marker for microglial activation following peripheral facial nerve axotomy. Although in the control mice the relative MalKO CD11b levels are slightly lower compared to the WT, they show no specific difference between WT and MalKO in the axotomised mice (Fig. 13). Also the expected elevation of CD11b protein levels in WT mice does not take place. This might be the case due to the choice of a too short observation time as well as procedural difficulties in the experiment and also would need to be repeated with bigger sample sizes.

4 Discussion

The results of this thesis will be briefly summarised as follows: MalKO mice show a delayed and impaired functional recovery of whisker movement in a 31 days period compared to the WT mice after peripheral facial nerve axotomy. In agreement with this data it has also been shown, that the motoneuron loss in the facial nucleus is significantly higher in MalKO mice than in WT mice. Additionally we observed increased levels of GFAP as a marker for astrocyte activation in axotomised MalKO mice compared to WT mice.

4.1 Functional recovery of whisker movement after peripheral facial nerve axotomy

In my project functional recovery of whisker movement and vibration was observed during a period of 31 days post peripheral facial nerve axotomy. It was estimated by comparing movement and vibration of the ipsilateral (injured) side with the contralateral (non-injured) side. Recovery was progressing nearly parallel in WT and MalKO mice right up to day 15. From there on a clear deterioration of functional recovery was observed in MalKO mice whereas the regeneration progressed in WT mice. Kamijo et al. [67] and others have shown, that after peripheral facial nerve crush mice recovered fully within 13 days. In facial nerve-transected animals the recovery time for full recovery was observed to be more than 10 weeks [71]. Within the 31 days of observation, the trend shown in WT mice recovery follows this findings. Additionally to the peak in astrocytic activation around day 14 after peripheral facial nerve axotomy in mice, a peak in both, neuronal cell death [74] and acti-

vated T-Lymphocyte infiltration [72, 44] have been observed. This occurs despite an intact Blood Brain Barrier (BBB) and specifically only in areas of degenerating neurons and activated phagocytic microglia [44]. The lymphocytic infiltration was also accompanied by a peak in the expression of interleukin-1 beta (IL-1β), tumor necrosis factor-alpha (TNFα) and interferon-gamma (IFNγ). Expression levels of those proinflammatory cytokines - mainly IL-1β and TNFα - have been shown to play a key role in recruiting CD3+ T-lymphocytes into the facial nucleus after peripheral nerve axotomy [72]. Different levels of those cytokines and different levels of CD3+ T-cells in MalKO mice compared to WT mice might present an explanation for the deterioration in functional recovery in MalKO-mice from day 15 on. Two possible explanations would be either a higher proinflammatory response, creating an increase in neuronal cell death or a lower response in cell survival associated pathways. Additionally it has been shown that inflammation is needed for regeneration [73]. Complete inhibition of inflammation has been shown to be extremely detrimental for regenerative processes and neuronal survival. The determination of the levels of the proinflammatory cytokines and CD3+ T-cell infiltration in the MalKO mouse facial nucleus, following peripheral facial nerve axotomy remain to be elucidated.

4.2 Neuronal cell death is higher in MalKO mice than in WT-mice

After observing functional recovery during 31 days axotomised mice were sacrificed and brain-slices were prepared at the level of the facial nuclei, stained with cresyl violet to study neuronal death in the facial nucleus after peripheral nerve axotomy. The sham-operated controls did not display any significant differences between the ipsilateral and the contralateral uninjured side. Also there was only a marginal insignificant difference in the absolute numbers of neurons in the facial nucleus between normal non injured MalKO and WT mice. Other studies in adult mice have shown degeneration of 20-35% of motoneurons in the facial nucleus after peripheral facial nerve transsection [74, 75]. Our own numbers of neuronal death in WT

mice are higher but stable at 40% ± 5% (mean ± SD; n=3) which might be due to methodological differences. In MalKO mice we have found a small but very consistent reduction of cell survival of 10% to 50% ±5% (mean ± SD; n=3) confirming the observation of impaired functional recovery in MalKO mice. MAL is a key player in the activation of NFκB, which is a major protein complex, controlling the transcription of a number of proinflammatory cytokines. NFκB plays also a role in modulating nerve regeneration following peripheral nerve injury [76]. Within the experimental context described above one can argue that in our model the lack of MAL signalling has an influence on peripheral nerve regeneration [77].

Our controls of Sham operated WT as well as MalKO mice show no signs for neuronal cell death in the facial nucleus, confirming the method of peripheral facial nerve axotomy as not interfering in motoneuron survival.

4.3 GFAP, Shp-1, CD11b, IRAK-1

Our experiments have shown an increase in GFAP levels after peripheral facial nerve injury in WT. This indicates - in accordance with the literature [42] - activation of astrocytes. We have observed a significantly higher expression of GFAP in MalKO mice, following the lesion, which is certainly an indication of stronger inflammatory response.

Horvat et al.[78] have shown, that SHP-1 is upregulated in activated microglia and astrocytes after peripheral nerve injury. Whereas in adult moth eaten viable (mev/mev) mice, known to have a reduced SHP-1 activity, a strong astrocytic activation (verified by GFAP-levels) but neither number nor morphology of microglia seemed to be modified. These findings are in accordance with our own results where a higher astrocytic activation takes place (indicated by increased GFAP-levels) in MalKO mice, where we simultaneously observe lower levels of SHP-1. At the same time the results for CD11b as a marker for microglial activation were not significant in any direction in MalKO mice. In WT mice there seems to be a trend to elevated protein levels for CD11b, although further experiments will be necessary to verify this trend. One possible explanation might be the short term observation of the

early signals at 2, 4 and 8 days, where the most intense peak for glial activation has been shown to be found between day 8 and 14 [42]. There might also be no clear trend visible, as these experiments have been done with only 3 mice per group, and a larger set of animals should be used in further investigations to get more statistically significant data.

It could be hypothesised that MAL plays a role in activating Shp-1, which would explain the decreased Shp-1 levels in MalKO mice. Indeed MAL contains an immunoreceptor tyrosine-based inhibition motif (ITIM), that is a conserved sequence of amino acids (S/I/V/LxYxxI/V/L) that is found in membrane bound and cytoplasmic molecules. ITIM motifs can be phosphorylated by members of the Src kinase family. Phosphorylated ITIMs can then recruit other enzymes such as the phosphotyrosine phosphatases SHP-1 and SHP-2, or the inositol-phosphatase called SHIP. Consequently, in our model system the lack of MAL in MalKO mice may be responsible for the lower levels of SHP-1 observed [79].

IRAK-1 is a kinase known to be a negative regulator of NFκB (REF). NFκB in turn is important for inflammatory responses in the CNS including astrocyte activation. The fact that we observed significantly elevated GFAP levels in MalKO mice compared to WT mice in addition to lower levels of IRAK-1 expression is consistent with a possible stronger inflammatory response. Strong NFkB activation - due to a lower regulatory influence of IRAK-1 - might therefore be the reason why we observed reduced functional recovery in MalKO mice.

As Raivich et al. [72] have shown in WT-mice, the NFκB pathway and secretion of cytokines play a vital role in the functional recovery following peripheral facial nerve axotomy. This inflammatory response appears to be important for neuronal cell survival and recovery as shown by Schwartz et al.[73] who has found protection of secondary neuronal degeneration after optical nerve crush by autoimmune T-cells. The peak of T-cell infiltration into the injured brain occurs around day 14 following the lesion where they aggregate around neuronal debris surrounded by phagocytic microglia. This correlates with the rapid regression in functional recovery of whisker movement in MalKO mice after day 15 post axotomy in our setup.

One could hypothesise that the absence of Mal leads to impaired NFκB activa-

tion and subsequently abolished or at least delayed and limited excretion of proinflammatory cytokines (IL1β, TNFα, IFNγ) resulting in insufficient recruitment of T-cells [72]. More likely the balance between inflammatory and protective response is severely disturbed by an increased inflammatory response, creating more neurodegenerative damage. Interestingly Kilic et al. [80] has reported a protective effect of TLR-4 deficiency in axotomy induced neurodegeneration in retinal ganglion cell axotomy in TLR4 deficient mice. Though this might be due to the observation period of only 14 days, where in our setting recovery just started to discontinue in MalKO mice.

Figure 15 depicts a hypothetical model based on our results, presenting a possible explanation for the impaired functional recovery and increased neuronal cell death in MalKO mice after peripheral facial nerve axotomy.

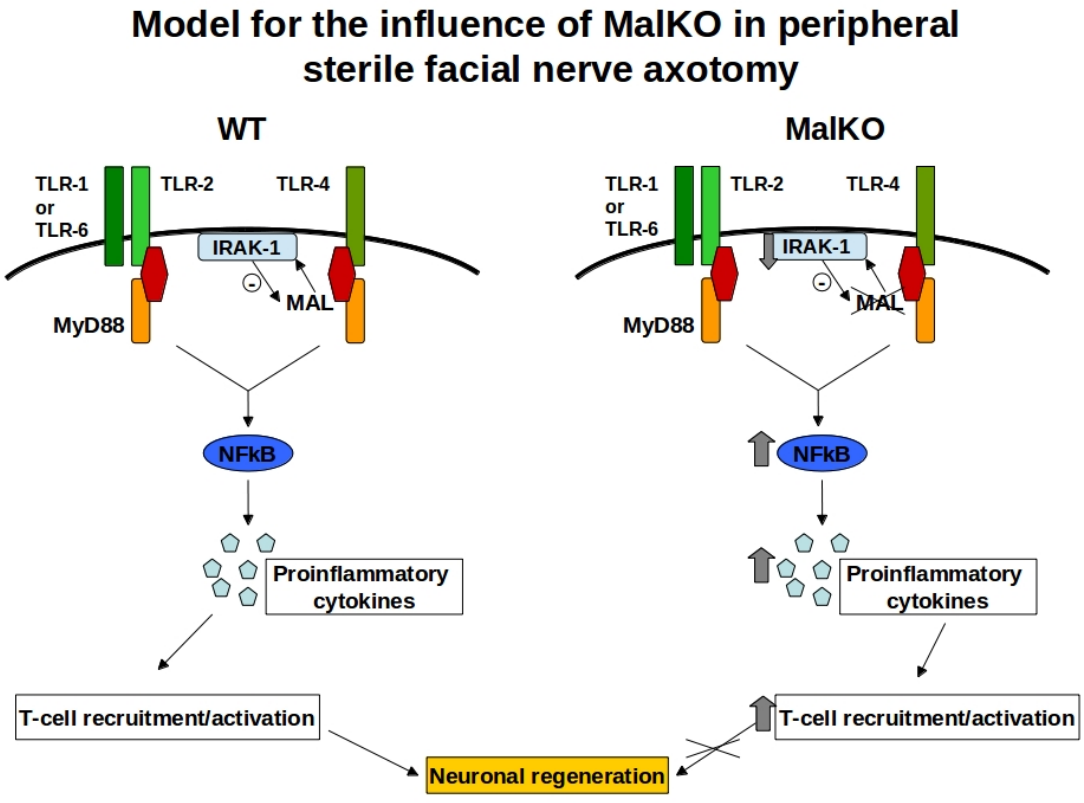

Figure 15: Depiction of a hypothetical model which would result in lower functional recovery and decreased neuronal survival in MalKO mice and is supported by our experimental results. Therefore the decreased levels of IRAK-1 found in MalKO mice might lead to increased NFκB activation, followed by a more severe inflammatory response, which would lead to significantly increased neuronal cell damage, thus preventing functional recovery and decreasing neuronal regeneration.

Therefore, with the inhibiting effects of IRAK-1 on NFkB activation no longer existing, one could assume a higher NFκB activation, which would be leading to an enhanced release of mainly proinflammatory cytokines. This fact, possible combined with a stronger cytotoxical T-cell recruitment and activation would necessarily lead to increased neuronal cell death and therefore naturally to decreased recovery in MalKO mice. The actual levels for NFκB and proinflammatory cytokines remain to be determined in further experiments as well as the amount of infiltrating T-cells.

4.4 Conclusions

MAL / TIRAP is a crucially important signalling molecule for TLR2 and TLR4 leading to NFKB activation and proinflammatory cytokines secretion.

Data produced in this work shows that MAL may play a role in facial motoneuron survival, peripheral facial nerve regeneration, facial nerve functional recovery and CNS glial activation following sterile Facial nerve peripheral lesion.

Our work raised three fundamental questions:

First, how can CNS glia "sense danger" and become activated following peripheral nerve injury that has occurred remotely from the CNS?

Second, what is the nature of the "signals" involved in glial activation in response to nerve injury?

Third, how do these "signals" interact with glial cells and control their activation state and function?

Further studies should be performed to gain a better understanding of the role of MAL in the mechanisms underlying CNS inflammation and nerve regeneration following peripheral nerve injury.

Bibliography

[1] Piao W., Song C., Chen L.M., Fitzgerald K.A., O'Neill L.A., Medvedev A.E.; Tyrosine Phosphorylation of MyD88 Adapter-like (MAL) is Critical for Signal Transduction and Blocked in Endotoxin Tolerance; The Journal of Biological Chemistry 2008; Vol 286, No. 6, pp 3109-3119

[2] O'Neill L.A.J., Bowie A.G.; The family of five: TIR-domain-containing adaptors in Toll-like receptor signalling; Nature Reviews Immunology (2007), Vol. 7, pp 353-364

[3] Aderem A, Ulevitch RJ.; Toll-like receptors in the induction of the innate immune response.; Nature. 2000 Aug 17;406(6797):782-7.;

[4] Takeda K., Kaisho T., Akira S.; Toll-like receptors.; Annu. Rev. Immunol. (2003), 21:335-76. Epub 2001 Dec 19.

[5] Wang J., Shao Y., Bennett T.A., Schankar R.A., Wightman P.D., Reddy L.G.; The functional effects of physical interactions among Toll-like receptors 7, 8, and 9; J. Biol. Chem. (2006) 281, 37427–37434;

[6] Hasan U, Chaffois C, Gaillard C, Saulnier V, Merck E, Tancredi S, Guiet C, Brière F, Vlach J, Lebecque S, Trinchieri G, Bates EE.; Human TLR10 is a functional receptor, expressed by B cells and plasmacytoid dendritic cells, which activates gene transcription through MyD88.; J Immunol. 2005 Mar 1;174(5):2942-50.

[7] Yarovinsky F, Zhang D, Andersen JF, Bannenberg GL, Serhan CN, Hayden MS, Hieny S, Sutterwala FS, Flavell RA, Ghosh S, Sher A (2005) TLR11 activation of dendritic cells by a protozoan profilin-like protein. Science 308:1626–1629

[8] Zhang D., Zhang G., Hayden M.S., Greenblatt M.B., Bussey C., Flavell R.A. et al.; A toll-like receptor that prevents infection by uropathogenic bacteria; Science, 303 (2004), pp. 1522–1526

[9] Yarovinsky F., Zhang D., Andersen J.F., Bannenberg G.L., Serhan C.N., Hayden M.S. et al.; TLR11 activation of dendritic cells by a protozoan profilin-like protein; Science, 308 (2005), pp. 1626–1629

[10] Jeyaseelan S., Manzer R., Young S.K., Yamamoto M., Akira S., Manson R.J., Worthen G.S.; Toll-IL-1 receptor domain-containing adaptor protein is critical for

early lung immune responses against Escherichia coli lipopolysaccharide and viable Escherichia coli.; J. Immunol. (2005), 175, 7484–7495;

[11] Jeyaseelan S., Young S.K., Yamamoto M., Arndt P.G., Akira S., Kolls J.K., Worthen G.S.; Toll/IL-1R domain-containing adaptor protein (TIRAP) is a critical mediator of antibacterial defense in the lung against Klebsiella pneumoniae but not Pseudomonas aeruginosa.; J. Immunol. (2006), 177, 538–547;

[12] Togbe D., Aurore G., Noulin N., Quesniaux V.F., Schnyder-Candrian S., Schnyder B., Vasseur V., Akira S., Hoebe K., Beutler B., Ryffel B., Couillin I.; Nonredundant roles of TIRAP and MyD88 in airway response to endotoxin, independent of TRIF, IL-1 and IL-18 pathways.; Lab. Invest. (2006), 86, 1126–1135;

[13] Sakata Y., Dong J.W., Vallejo J.G., Huang C.H., Baker J.S., Tracey K.J., Tacheuchi O., Akira S., Mann D.L.; Toll-like receptor 2 modulates left ventricular function following ischemia-reperfusion injury.; Am. J. Physiol. Heart Circ. Physiol. (2006), 292, H503–H509;

[14] Yamamoto M, Sato S, Hemmi H, Sanjo H, Uematsu S, Kaisho T, et al; Essential role for TIRAP in activation of the signalling cascade shared by TLR2 and TLR4; Nature (2002), 420(6913):324–9;

[15] Dunne A, Ejdeback M, Ludidi PL, O'Neill LA, Gay NJ; Structural complementarity of Toll/interleukin-1 receptor domains in Toll-like receptors and the adaptors Mal and MyD88; J Biol Chem (2003), 278(42):41443–51;

[16] Kagan J. C., Medzhitov R.; Phosphoinositide-mediated adaptor recruitment controls Toll-like receptor signaling; Cell (2006), 125, 943–955;

[17] Nakagawa R., Naka T., Tsutsui H., Fujimoto M., Kimura A., Abe T., Seki E., Takeuchi O., Takeda K., Akira S., Yamanishi K., Kawase I., Nakanishi K., Kishimoto T.; SOCS-1 participates in negative regulation of LPS responses; Immunity (2002); 17, 677–687;

[18] Kinjyo I., Hanada T., Inagaki-Ohara K., Mori H., Aki D., Ohishi M., Yoshida H., Kubo M., Yoshimura A.; SOCS1/JAB is a negative regulator of LPS-induced macrophage activation. Immunity (2002), 17, 583–591;

[19] Horng T., Barton G. M., Flavell R. A., Medzhitov R.; The adaptor molecule TIRAP provides signalling specificity for toll-like receptors; Nature (2002), 420, 329–333;

[20] Yamamoto M., Sato S., Hemmi H., Sanjo H., Uematsu S., Kaisho T., Hoshino K., Takeuchi O., Kabayashi M., Fujita T., Takeda K., Akira S.; Essential role for TIRAP in activation of the signalling cascade shared by TLR2 and TLR4; Nature (2002), 420, 324–329;

[21] Tammy Kielian; Toll-Like Receptors in Central Nervous System Glial Inflammation and Homeostasis; Review, Journal of Neuroscience Research, 83: 711-730 (2006)

[22] Miggin S.M., Palsson-McDermott E., Dunne A., Jefferies C., Pinteaux E., Banahan K. et al.; NF-kappaB activation by the Toll-IL-1 receptor domain protein MyD88 adapter-like is regulated by caspase-1; Proc Natl Acad Sci USA (2007); 104(9):3372–7;

[23] Gray P., Dunne A., Brikos C., Jefferies C.A., Doyle S.L., O'Neill L.A.; MyD88 adapter-like (Mal) is phosphorylated by Bruton's tyrosine kinase during TLR2 and TLR4 signal transduction; J Biol Chem (2006), 281(15):10489–95;

[24] Piao W., Song C., Chen H., Wahl L.M., Fitzgerald K.A., O'Neill L.A. et al; Tyrosine phosphorylation of MyD88 adapter-like (Mal) is critical for signal transduction and blocked in endotoxin tolerance; J Biol Chem (2008), 283(6):3109–19;

[25] Gray P., Dunne A., Brikos C., Jefferies C.A., Doyle S.L., O'Neill L.A.J.; MyD88 Adapter-like (MAL) Is Phosphorylated by Bruton's Tyrosine Kinase during TLR2 and TLR4 Signal Transduction; The Journal of Biological Chemistry Vol. 281, No 15, pp 10489-10495;

[26] Khor CC, Chapman SJ, Vannberg FO, Dunne A, Murphy C, Ling EY, Frodsham AJ, Walley AJ, Kyrieleis O, Khan A, Aucan C, Segal S, Moore CE, Knox K, Campbell SJ, Lienhardt C, Scott A, Aaby P, Sow OY, Grignani RT, Sillah J, Sirugo G, Peshu N, Williams TN, Maitland K, Davies RJ, Kwiatkowski DP, Day NP, Yala D, Crook DW, Marsh K, Berkley JA, O'Neill LA, Hill AV; A MAL functional variant is associated with protection against invasive pneumococcal disease, bacteremia, malaria and tuberculosis; Nat Genet. 2007 Abr; 39(4):532-8.

[27] Jefferies, C. A., Doyle, S., Brunner, C., Dunne, A., Brint, E., Wietek, C., Walch, E., Wirth, T., and O'Neill, L. A. (2003) J. Biol. Chem. 278, 26258 –26264

[28] Horwood, N. J., Mahon, T., McDaid, J. P., Campbell, J., Mano, H., Brennan, F. M., Webster, D., and Foxwell, B. M. (2003) J. Exp. Med. 197, 1603–1611

[29] Dunne A, Carpenter S., Brikos C., Gray P., Strelow A., Wesche H., Morrice N., O'Neill L.A.J.; IRAK1 and IRAK4 Promote Phosphorylation, Ubiquitination, and Degradation of MyD88 Adaptor-like (MAL); The Journal of Biological Chemistry Vol. 285, No. 24, pp 18276-18282, June 11, 2010;

[30] Verstak B, Nagpal K, Bottomley SP, Golenbock DT, Hertzog PJ, Mansell A; MyD88 adapter-like (MAL)/TIRAP interaction with TRAF6 is critical for TLR2- and TLR4-mediated NF-kappaB proinflammatory responses; J Biol Chem. 2009 Sep 4;284(36):24192-203. Epub 2009 Jul 10;

[31] Araque A., Parpura V., Sanzgiri R.P., Haydon P.G.; Tripartite synapses: glia, the unacknowledged partner; Trends Neurosci (1999), 22:208-215;

[32] Carmignoto G.; Reciprocal communication systems between astrocytes and neurones; Prog Neurobiol (2000), 62:561-581;

[33] Ridet J.L., Malhotra S. K., Privat A., Gage F.H.; Reactive astrocytes: cellular and molecular cues to biological function; Trends Neurosci (1997), 20:570-577;

[34] Dong Y., Beneviste E.N.; Immune function of astrocytes; Glia (2001), 36:180-190;

[35] Giaume C, Venance L.; Gap junctions in brain glial cells and development; Perspect Dev Neurobiol (1995) 2:335-345

[36] Temburni M.K., Jacob J.H.; New functions for glia in the brain; PNAS, Vol. 98 (2001), No. 7, pp 3631-3632

[37] Fileds R. Douglas, Stevens-Graham Beth, New Insights into Neuron-Glia Communication, Science, 18. Oct. 2002, Vol 298

[38] Verkhratsky A., Steinhauser C.; Ion channels in glial cells; Brain Res Brain Res Rev 2000;32(2–3):380–412;

[39] Butt Arthur M.; ATP: A ubiquitous gliotransmitter integrating neuron-glial networks; Review; Seminars in Cell and Developmental Biology 22, 2011, 205-213);

[40] Cullheim S., Thams S.; The microglial networks of the brain and their role in neuronal network plasticity after lesion; Brain Research Reviews 55 (2007), pp 89 – 96

[41] Metea M.R., Newman E.A.; Calcium signaling in specialized glial cells; Glia 2006;54:650–5;

[42] Campos-Torres A., Vidal P.P., De Waele C.; Evidence for a Microglial Reaction Within the Vestibular and Cochlear Nuclei Following Inner Ear Lesion in the Rat; Neuroscience 92 (1999), No. 4, pp. 1475 – 1490

[43] Porter, J. T. McCarthy, K. D. (1997) Prog. Neurobiol. 51, 439–455.

[44] Raivich G., Jones L.L., Kloss C.U.A., Werner A., Neumann H., Kreutzberg G.W.; Immune Surveillance in the Injured Nervous System: T-Lymphocytes Invade the Axotomized Mouse Facial Motor Nucleus and Aggregate around Sites of Neuronal Degeneration; The Journal of Neuroscience, August 1, 1998, 18(15):5805-5816

[45] Escartin C., Bonvento G; Targeted activation of astrocytes: a potential neuroprotective strategy; Mol Neurobiol (2008) 38(3):231–41;

[46] Anderson M.F., Blomstrand F.; Blomstrand C., Eriksson P.S., Nilsson M.; Astrocytes and stroke: networking for survival? Neurochem Res (2003), 28: 293-305;

[47] Anderson M.F., Swanson R.A.; Astrocyte glutamate transport: review of properties, regulation, and physiological functions. GLia (2000), 32:1-14;

[48] Swanson R.A., Kauppinen T.M.; Astrocyte influences on ischemic neuronal death; Curr Mal Med (2004), 4:193-205;

[49] Pekny M., Nilsson M.; Astrocyte Activation and Reactive Gliosis; Glia (2005), 50: 427-434,

[50] Nimmerjahn A., Kirchhoff F., Helmchen F.; Resting microglial cells are highly dynamic surveillants of brain parenchyma in vivo; Science 2005;308(5726):1314–8.

[51] W. Liu, Y. Tang, J.Feng; Cross talk between activation of microglia and astrocytes in pathological conditions in the central nervous system; Life Sciences 89

(2011) 141-146;

[52] Giulian, D., Vaca, K., Corpuz, M.; Brain glia release factors with opposing actions upon neuronal survival; J. Neurosci. (1993), 13,29–37.

[53] Thery, C., Chamak, B., Mallat, M.; Cytotoxic effects of brain macrophages on developing; Eur. J. Neurosci. (1991), 3, 1155–1164.

[54] Chao, C.C., Hu, S., Molitor, T.W., Shaskan, E.G., Peterson, P.K.; Activated microglia mediate neuronal cell injury via a nitric oxide mechanism; J. Immunol. (1992), 149, 2736–2741.

[55] Streit, W.J., Kreutzberg, G.W.; The response of endogenous glial cells to motor neuron degeneration induced by toxic ricin; J. Comp. Neurol. (1988) 268, 248–263.

[56] Matsumoto Y., Ohmori K., Fujiwara M.; Microglia and astroglial reactions to inflammatory lesions of experimental autoimmune encephalomyelitis in the rat central nervous system; J Neuroimmunol (1992), 37(1–2):23–33.

[57] Gatan E., Overmier B.J.; Inflammatory pathogenesis in Alzheimer's disease: biological mechanisms and cognitive sequeli; Neurosci Biobehav Rev (1999), 23(5):615–33;

[58] Colburn R.W., Deleo J.A., Rickman A.J., Yeager M.P., Kwon P., Hickey W.F.; Dissociation of microglial activation and neuropathic pain behaviors following peripheral nerve injury in the rat; J Neuroimmuology (1997), 79(2):163–75;

[59] Ramírez G., Toro R., Döbeli H., von Bernhardi R.; Protection of rat primary hippocampal cultures from A beta cytotoxicity by pro-inflammatory molecules is mediated by astrocytes; Neurobiol Dis (2005), 19(1–2):243–54;

[60] Herrera-Molina R., von Bernhardi R.; Transforming growth factor-beta 1 produced by hippocampal cells modulates microglial reactivity in culture; Neurobiol Dis (2005), 19(1–2):229–36;

[61] Huang W.C., Yen F.C., Shie F.S., Pan C.M., Shiao Y.J., Yang C.N., et al.; TGF-beta1 blockade of microglial chemotaxis toward Abeta aggregates involves SMAD signaling and down-regulation of CCL5; J Neuroinflammation (2010), 7:28;

[62] Graeber M.B., Lopez-Redondo F., Ikoma E., Ishikawa M., Imai Y., Nakajima K., Kreutzberg G.W., Kohsaka S.; The microglia/macrophage response in the neonatal rat facial nucleus following axotomy; Brain Res. (1998), 813:241-253;

[63] Streit W.J., Kreutzberg G.W., Response of endogenous glial cells to motor neuron degeneration induced by toxin ricin; J. Comp. Neurol. (1988), 268:248-263;

[64] Dai C.F., Kanoh N., Li K.Y., Wang Z.; Study on facial motoneuronal death after proximal or distal facial nerve transection; Am. J. Otol. (2000), 21:115-118;

[65] Moran L.B., Graeber M.B.; The facial nerve axotomy model; Review, Brain Research Reviews 44 (2004), 154-178;

[66] K.W.Ashwell; The adult mouse facial nerve nucleus: morphology and musculotopic organization; Journal of Anatomi (1982), 135, 3, pp. 531-538;

[67] Kamijo Y., Koyama J., Oikawa S., Koizumi Y., Yokouchi K., Fukushima N., Moriizumi T.; Regenerative process of the facial nerve: rate of regeneration of fibers and their bifurications; Neuroscience Research 46 (2003) 135-143

[68] Watson C.R., Sakai S., Armstrong W.; Org anization of the facial nucleus in the rat; Brain Behav. Evol. (1982), 20:19-28;

[69] Campos-Torres A., Touret M., Vidal P.P., Barnum S., De Waele C.; The Differential Response of Astrocytes Within the Vestibular and Cochlear Nuclei Followin Unilateral Labyrinthectomy or Vestibular Afferent Activity Blockade by Transtympanic Tetrodotoxin Injection in the Rat; Neuroscience 130 (2005), pp 853-865

[70] Laemmli U.K.; Cleavage of structural proteins during the assembly of the head of bacteriophage T4; Nature (1970), 227:680-685;

[71] Choi D, Raisman G.; Somatotopic organization of the facial nucleus is disrupted after lesioning and regeneration of the facial nerve: the histological representation of synkinesis.; Neurosurgery. 2002 Feb;50(2):355-62; discussion 362-3.

[72] Raivich G., Bohatschek M., Werner A., Jones L.L., Galiano M., Kloss C.U.A., Zhu X.Z., Pfeffer K., Liu Z.Q.; Lymphocyte Infiltration in the Injured Brain: Role of Proinflammatory Cytokines; Journal of Neuroscience Research 72:726-733 (2003)

[73] Moalem G., Leibowitz-Amit R., Yoles E., Mor F., Cohen I.R., Schwartz M.; Autoimmune T cells protect neurons from secondary degeneration after central nervous system axotomy; Nat Med. 1999 Jan;5(1):49-55.

[74] Möller J.C., Klein M.A., Haas S., Jones L.L., Kreutzberg G.W., Raivich G.; Regulation of thrombospondin in the regenerating mouse facial motor nucleus; Glia (1996), 17:121-132;

[75] Torvik A., Skjörten F.; Electron microscopic observations on nerve cell regeneration and degeneration after axon lesions. II. Changes in the glial cells; Acta Neuropathol (1971), 17:265-282;

[76] Verstrepen L., Bekaert T., Chau T.L., Taernier J., Chariot A., Beyaert R.; TLR-4, IL-1R and TNF-R signaling to NR-kappaB: variations on a common theme; Cell Mol Life Sci. (2008), Oct; 65(19):2964-78; Review;

[77] Smith D, Tweed C, Fernyhough P, Glazner GW.; Nuclear factor-kappaB activation in axons and Schwann cells in experimental sciatic nerve injury and its role in modulating axon regeneration: studies with etanercept.; J Neuropathol Exp Neurol. (2009) Jun;68(6):691-700.

[78] Horvat A., Schwaiger F.W., Hager G., Bröcker F., Streif R., Knyazev P.G., Ullrich A., Kreutzberg1 G.W.; A Novel Role for Protein Tyrosine Phosphatase SHP-1 in Controlling Glial Activationn in the Normal and Injured Nervous System; Journal of Neuroscience, February 1, 2001, 21(3):865–874

[79] Pinheiro da Silva F., Aloulou M., Benhamou M., Monteiro R.C.; Inhibitory ITAMs: a matter of life and death.; Trends in Immunology, Vol.29 No.8

[80] Kilic U., Kilic E., Matter C.M., Bassetti C.L., Hermann D.M.; TLR-4 deficiency protects against focal cerebral ischemia and axotomy-induced neurodegeneration; Neurobiology of Disease 31 (2008), 33-40;

[81] Ladeby R., Wirenfeldt M., Garcia-Ovejero D., Fenger C., Dissing-Olesen L., Dalmau I., Finsen B.; Microglial cell population dynamics in the injured adult central nervous system; Brain Research Reviews (2005), 48, 196-206;

Acknowledgements

First, I want to thank Univ.Doz. Dr. Monika Bradl, for being my supervisor at the University of Vienna and therefore for giving me the opportunity to do my thesis abroad and also for her efficient and quick email support.

I also would like to express my sincere gratitude and heartfelt thanks to Dr. Antonio Campos Torres DDS, MSc, PhD, my supervisor at the National University of Ireland, Maynooth (NUIM) who has been supporting me all through the practical work as well as the writing of this thesis. I want to thank him for his never ending patience, his excellent advice and the great humour he handles things with. Also I want to thank him for his contagious enthusiasm for science and for sharing his way of dealing with problems and experiments gone wrong as a learning experience. Also I really treasure all the - partly heated – discussions helping me to get a deeper understanding of the topic. He made my stay at the NUIM a great experience.

I am also very grateful to Prof. Paul Moynagh, Head of Biology Department for putting all his equipment and workspace in his lab to my use, as well as all the members of the lab for their support and advice over these 18 months. Additionally I would like to thank Mrs. Deirdre Daly, BSc., Technical Officer at the Animal facilities of the Institute of Immunology at NUIM for helping with the breeding.

A big thank you also goes to all my friends, the newly found ones in Ireland who provided great support and well needed distraction in stressful times and also helped me to understand the Irish and their culture a little bit better. And of course also big thanks to my friends from Austria for giving great online support and staying in touch, despite the physical distance.

Finally, I want to thank my family for all their support and encouragement, to go my way and for always providing a well meaning and patient ear to any stories, good or bad, and always giving good advice.

Curriculum Vitae

Name	Marion Nidetzky
Date of Birth	21. June 1981
Place of Birth	Vienna, Austria
Nationality	Austria

Education

March 2005 – September 2012	Molecular Biology, University of Vienna
October 1999 – February 2005	Applied Computer Sciences, Institute for Scientific Computing, University Salzburg
June 1999	*Matura* (written examinations: german, mathematics, english; oral examinations: french, religion, biology, chemistry) *BORG Oberstufenrealgymnasium*, Neumarkt am Wallersee, Austria (general university entry qualification)
September 1995 – June 1999	Grammar School *BORG* Oberstufenrealgymnasium, with a focus on music, Neumarkt am Wallersee, Austria

Employment and Work Experience

August – October 2002	*dm-drogerie markt GmbH + Co. KG* Computer Sciences Study related work experience in software development in the companies IT department

Research experience

February 2011 – June 2012	Master Thesis Institute of Immunologie, National University of Ireland, Maynooth; Ireland Prof. Paul Moynagh research group Dr. Antonio Campos-Torres
November 2010 – February 2011	Internship Institute of Immunologie, National University of Ireland, Maynooth; Ireland Prof. Paul Moynagh Research Group Dr. Antonio Campos-Torres The Pellino protein family
July – September 2009	Internship School of Biomolecular and Biomedical Sciences; Conway Institute; University College Dublin; Ireland Dr. Jana Haase Research Group Regulation of serotonin transporter gene expression by proinflammatory cytokines